2017-12-01

Understanding Community and Ecophysiology of Plant Species on the Colorado Plateau

Hannah Elizabeth Yokum
Brigham Young University

Understanding Community and Ecophysiology of Plant Species on the Colorado Plateau

Hannah Elizabeth Yokum

A thesis submitted to the faculty of
Brigham Young University
in partial fulfillment of the requirements for the degree of

Master of Science

Richard A. Gill, Chair
Samuel B. St. Clair
Ryan R. Jensen
David L. Hoover

Department of Biology

Brigham Young University

ABSTRACT

Understanding Community and Ecophysiology of Plant Species on the Colorado Plateau

Hannah Elizabeth Yokum
Department of Biology, BYU
Master of Science

The intensification of aridity due to anthropogenic climate change is likely to have a large impact on the growth and survival of plant species in the southwestern U.S. where species are already vulnerable to high temperatures and limited precipitation. Global climate change impacts plants through a rising temperature effect, CO_2 effect, and land management. In order to forecast the impacts of global climate change, it is necessary to know the current conditions and create a baseline for future comparisons and to understand the factors and players that will affect what happens in the future. The objective of Chapter 1 is to create the very first high resolution, accurate, park-wide map that shows the distribution of dominant plants on the Colorado Plateau and serves as a baseline for future comparisons of species distribution. If we are going to forecast what species have already been impacted by global change or will likely be impacted in the future, we need to know their physiology. Chapter 2 surveys the physiology of the twelve most abundant non-tree species on the Colorado Plateau to help us forecast what climate change might do and to understand what has likely already occurred.

Chapter 1. Our objective was to create an accurate species-level classification map using a combination of multispectral data from the World View-3 satellite and hyperspectral data from a handheld radiometer to compare pixel-based and object-based classification. We found that overall, both methods were successful in creating an accurate landscape map. Different functional types could be classified with fairly good accuracy in a pixel-based classification but to get more accurate species-level classification, object-based methods were more effective (0.915, kappa coefficient=0.905) than pixel-based classification (0.79, kappa coefficient=0.766). Although spectral reflectance values were important in classification, the addition of other features such as brightness, texture, number of pixels, size, shape, compactness, and asymmetry improved classification accuracy.

Chapter 2. We sought to understand if patterns of gas exchange to changes in temperature and CO_2 can explain why C_3 shrubs are increasing, and C_3 and C_4 grasses are decreasing in the southwestern U.S. We conducted seasonal, leaf-level gas exchange surveys, and measured temperature response curves and A-C_i response curves of common shrub, forb, and grass species in perennial grassland ecosystems over the year. We found that the functional trait of being evergreen is increasingly more successful in climate changing conditions with warmer winter months. Grass species in our study did not differentiate by photosynthetic pathway; they were physiologically the same in all of our measurements. Increasing shrub species, *Ephedra viridis* and *Coleogyne ramosissima* displayed functional similarities in response to increasing temperature and CO_2.

Keywords: climate change, drylands, ecophysiology, photosynthesis, plant sensitivity, World View-3, l, object-based classification, pixel-based classification

ACKNOWLEDGEMENTS

I would like to thank the U.S. Geological Survey for their generous support, both financially and scientifically for the project. On the USGS team is Dr. David Hoover who assisted me personally as a member on my committee, reading drafts and advising me on methodology, species identification, and site-specific information. He created the R program, R Goldy, for determining stability with the Li-COR machines as well as width to surface area conversions for major species so I wouldn't have to clip and measure leaf surface area for all of the species. The USGS also provided the satellite imagery for the second chapter along with help from Dr. Miguel Villarreal. I would like to recognize a few of the many professors at BYU who offered personal support and mentoring to me along the journey: Dr. Roger Koide, Dr. Jerry Johnson, Dr. Steve Schill, Dr. Steve Peterson, and Dr. Randy Larsen. I would like to thank Dr. Ryan Jensen for his remote sensing and GIS expertise that was necessary for the mapping and classification of the imagery. A big thanks to Dr. Samuel St. Clair for his ecophysiology experience and editing mastery. And finally, so much recognition goes to Dr. Richard Gill, my adviser, for the funding, project ideas, support, mentoring and the hundreds of edits he patiently endured. This experience has brought both personal and scientific growth and I am grateful for all of the mentoring and friendship shown to me along the way.

TABLE OF CONTENTS

TITLE PAGE i

ABSTRACT ii

ACKNOWLEDGEMENTS iii

TABLE OF CONTENTS iv

LIST OF TABLES vi

LIST OF FIGURES vii

Chapter 1: 1

Abstract *1*

Introduction *2*

Methods *6*

Site Description 6

Study Design 8

Climate Data 9

Photosynthetic Gas Exchange Measurements 10

Leaf-level Photosynthesis Point Measurements 10

A-C_i Response Curves 11

Temperature Response Curves 11

Statistical analyses 12

Results *13*

Precipitation and Temperature Measurements 14

Seasonal Gas Exchange Measurements 15

Temperature Response Curves and Optima 17

A-C_i Response Curves 20

Grouping Species by General Strategies for Success 22

Discussion *25*

Seasonal Gas Exchange Measurements 26

Temperature and CO_2 Response Curves 28

Grouping of General Strategies for Success 30

Conclusions *30*

References *32*

Chapter 2: 38

Using Very High Resolution (VHR) satellite Imagery to Create an Accurate, Species-level Baseline Map in Canyon Terrain 38

Abstract *38*

Introduction *39*
Remote Sensing 40
Image Classification 42
Methods *46*
Site Description 46
Image Pre-processing 46
Reflectance curves and pixel-based classification 48
Ground Reference Data 49
Comparison of Approaches 50
Spectral Differentiation 50
Object oriented classification 52
Important Features in Object-based classification 53
Accuracy Assessment 54
Results *55*
Reflectance Curves and Pixel-based Classification 55
Compare pixel-level classification to object-level classification 55
Important Features in Object-based Classification 56
Discussion *63*
Classification Accuracy 63
Limitations of the method 65
Implications 66
References *67*
Supplementary Information 76
Chapter 1 ..... *76*
Chapter 2 ..... *77*

LIST OF TABLES

Chapter 1: 1

Table 1 Species measured in the study 9
Table 2 Species Spring maximum photosynthetic rate and optimum temperatures 19
Table 3 ANOVA results 23

Chapter 2: 38

Table 1 Species measured 48
Table 2 Pixel-based confusion matrix 59
Table 3 Object-based confusion matrix 59
Table 4 Class separation distance matrix 61
Table 5 Object overlap values 62
Table 6 Other features that can be used to increase separation distance 62

Supplementary Information 76

Chapter 1 ..... *76*
Table S1 Point measurements for photosynthetic rate 76

Chapter 2 ..... *77*
Table S1 Classification Sample Editor 83

LIST OF FIGURES

Chapter 1: 1

Figure 1 7
Figure 2 15-year average precipitation and monthly precipitation values graphed 15
Figure 3 Point photosynthetic measurements 17
Figure 4 Temperature Response Curves 18
Figure 5 Temperature optima days over the past 15 years 20
Figure 6 A-Ci curves 22
Figure 7 Clustering of species by similar traits 24
Figure 8 Important variables in clustering 25

Chapter 2: 38

Figure 1 Study site 47
Figure 2 Spectral signatures 49
Figure 3 Spectral signature decision tree 50
Figure 4 Image processing methods 51
Figure 5 Classification map 58

Supplementary Information 76

Chapter 2 ..... *77*
Figure S1 Original image and classification 77
Figure S2 Chelser Park Classification 78
Figure S3 Zoomed in Chesler Park Classification 79
Figure S4 Shrub to grass interface in Chesler Park 80
Figure S5 Virginia Park classification 81
Figure S6 Visitor Center classification 82

Chapter 1:

Plant sensitivities to temperature and CO_2 contribute to competitive advantages on the Colorado Plateau

Abstract

Plant species responses to changing climate in dryland ecosystems are shaped by their ability to fix carbon dioxide while avoiding water loss. This tradeoff is influenced by global climate change, including increases in atmospheric CO_2 and temperature and more variable precipitation patterns. We sought to understand if patterns of gas exchange to changes in temperature and CO_2 can identify possible competitive advantages for C_3 shrubs over C_3 and C_4 grasses in the changing climate of the southwestern U.S. To test this, we conducted seasonal, leaf-level gas exchange surveys, and measured temperature response curves and A-C_i response curves of dominant shrub, forb, and grass species in perennial grassland ecosystems on the Colorado Plateau. We found that both C_3 and C_4 grass species were physiologically identical to each other and were more sensitive to changes in CO_2 concentrations compared to shrubs and forbs. Evergreen C_3 shrubs were functionally similar and were able to maintain photosynthetic activity throughout winter when minimum temperature requirements were met. Over the last fifteen years, there has been a steady increase in the number of winter days when temperatures are warm enough for net positive photosynthetic activity in C_3 shrub species. During these winter months, C_3 and C_4 competitor grass species are senesced so shrubs have limited competition for resources. Grass species had higher photosynthetic rates and temperature optima, but increasing, evergreen C_3 shrub species were consistent with wider optimum conditions.

Key-words: A-Ci curves, climate change, cold desert, dryland, ecophysiology, photosynthesis, temperature response curves

Introduction

Plant species responses to changing climate in dryland ecosystems is shaped by their ability to fix carbon dioxide while avoiding water loss (Amthor 1995; Blumenthal *et al.* 2016). This tradeoff is influenced by climate change, including increases in atmospheric CO_2 and temperature and more variable precipitation patterns in the southwestern United States (Easterling *et al.* 2000; Sun *et al.* 2007; Diffenbaugh *et al.* 2005; Christensen *et al.* 2007). These abiotic changes affect the ability of plants to capture carbon efficiently, (Shaw *et al.* 1998; Sheffield and Wood 2008b, a; Christensen *et al.* 2007) especially in regions where species are already vulnerable to high temperatures and limited precipitation (Karl *et al.* 2009). Understanding species sensitivities to climate change will allow more accurate comparisons of plant species vulnerabilities and projections of shifts in community density, distribution, and diversity (Shaw *et al.* 1998; Adler 2008; Algar *et al.* 2009; Sheppard & Stanley 2014; Fay *et al.* 2015).

Photosynthesis is the primary physiological process that drives plant growth and influences many other plant processes. It is also strongly affected by changing abiotic conditions, such as rising temperature and atmospheric CO_2 concentration, making it an ideal indicator of the effect of climate on plant species (Yin & Struik 2009). Plant photosynthetic capacity has been shown to strongly correlate with growth rates and contribute to competitive advantages making it a useful proxy for plant success under future climate scenarios (Lusk & Del Pozo 2002; Lusk *et al.* 2003). Photosynthetic responses to CO_2 concentration and temperature indicate biochemical function (limitations in the availability of the enzyme Rubisco or substrate RUBP) and stomatal regulation, and are therefore important for understanding biological changes in the plant (Davies 1998; Sharkey *et al.* 2007; Momen 2015; Sigut *et al.* 2015; Song *et al.* 2016).

Elevated atmospheric CO_2 concentration can stimulate plant photosynthesis, increase light efficiency, improve plant-water use efficiency, reduce stomatal conductance and transpiration, increase the transfer of C from plants to soil, and inhibit plant respiration (Idso *et al.* 1993; Callaway *et al.* 1994; Gunderson and Wullschleger 1994; Jackson *et al.* 1994; Amthor 1995; Polley *et al.* 2013). Elevated CO_2 concentrations might also bring about no changes in plant photosynthesis if individuals assimilate to the changes. Both CO_2 concentration and photosynthetic rate are highly dependent on leaf temperature. Researchers have found that climate warming can either stimulate (Apple *et al.* 2000; Huxman *et al.* 1998; Liang *et al.* 2013; Niu *et al.* 2008a), constrain (Jochum *et al.* 2007; Xu & Zhou 2005), or bring about no noticeable change (Newingham *et al.* 2014) in plant photosynthetic rates. Tolerance to high temperatures and a higher temperature optima indicate species better equipped for ecosystem warming (Ghouil *et al.* 2003; Heskel *et al.* 2016). Tolerance for a wide range of temperature optima allows the plant to perform at peak, or near peak, photosynthesis rates over a larger range of temperatures. Increases in temperature have been shown to reduce the rate of photosynthesis and density in the landscape in one shrub species while benefiting another shrub species (Shaw *et al.* 1998).

Plant seasonal gas exchange measurements and response curves for changing CO_2 and temperature are effective ways to use photosynthetic rates to characterize species-specific sensitivities to climate change (Ainsworth *et al.* 2003; Wullschleger *et al.* 2002; Dawson *et al.* 2004; Sheppard & Stanley, 2014; Song *et al*. 2016). Comparisons between instantaneous measures of leaf gas exchange across different CO_2 concentrations and temperature indicate how short term responses of leaf-level performance relate to more integrated responses to climate change (Shaw *et al.* 1998; Romero & Botia 2005; Wullschleger *et al.* 2002; Song *et al.* 2016).

Analysis of A-C_i curves, the response of net photosynthesis (A) to varying intercellular CO_2 concentrations (C_i), has been used to distinguish between diffusional and biochemical limitations to photosynthesis (Ainsworth *et al.* 2003; Hu *et al.* 2010). Maximum velocity of carboxylation of Rubisco (V_{cmax}) and maximum electron transport rate (J_{max}) have been shown to increase with warmer temperatures and indicate differences in nitrogen and phosphorus availability making them an important measure of sensitivity (Walker *et al*. 2014). Temperature response curves indicate short-term changes in photosynthetic rate with increasing temperature. They can be used to determine ideal temperature ranges for growth and photosynthesis of species as well as functional groups (Ziska 2001; Ghouil *et al.* 2003). Increases in photosynthetic rate in elevated CO_2 and temperature conditions is well documented for both C_3 and C_4 species (Bowes 1993; Gunderson and Wullschleger 1994; Amthor 1995; Drake *et al.* 1997; Herrick and Thomas 1998; Pataki *et al.* 1998; Wand *et al.* 1999; Wullschleger *et al.* 2002; Ainsworth *et al.* 2003; Sholtis *et al*. 2004; Warren *et al.* 2015; Duffy & Chown 2016). Based on the carboxylation kinetics of the C_3 pathway, C_3 species have been shown to have an increase in assimilation rates in high CO_2 conditions relative to C_4 species (Valerio *et al.* 2013; Cunniff *et al.* 2016; Sage and Khoshravesh 2016). C_4 species have been shown to respond more favorably to increased temperatures, still respond to increasing CO_2, and be more resilient to environmental stress compared to C_3 species (Pearcy & Ehleringer 1984; Wand *et al.* 1999; Wang *et al.* 2012; Tooth and Leishman 2013; Valerio *et al.* 2013; Cunniff *et al.* 2016; Duffy & Chown 2016; Hao *et al.* 2017). Seasonal gas exchange measurements identify important seasons for growth, the number of days over winter when plants are photosynthetically active, seasons that are most influenced by climate change in the region, and the species that benefit from the changing conditions. We expect warmer winter months, predicted in climate change projections, to benefit shrubs only if they are

photosynthetically active during winter months. Monitoring species sensitivities to changing abiotic conditions can identify instances of plant stress and acclimation. We use these parameters to determine how abiotic factors associated with climate change are influencing photosynthesis rates in plants and if there are traits in common between different groups of species.

The Colorado Plateau is an ideal place to evaluate plant sensitivity to environmental seasonality because there are large seasonal changes in temperature, a clear directional change in climate, and several key species that have been shown to vary in their responsiveness to climate change. Previous studies from the region have found that species with a C_4 photosynthetic pathway benefit in changing climate conditions (Munson *et al.* 2011a; Duffy & Chown 2016). In the case of shrubs however, C_3 shrubs, not C_4 shrubs, were more are resistant to drought (Hoover *et al.* 2015). Another study found that, when faced with a 35% drought press, C_4 grasses were sensitive to drought across all measured variables, and the C_3 shrubs had little to no response to drought conditions (Hoover *et al.* 2017). Over a twenty-year period, a common C_3 shrub species found in perennial grasslands, *Ephedra viridis*, showed some increase in its canopy cover with increasing mean annual temperature, while C_3 grasses showed sharp declines. This suggests that plant sensitivity to temperature is potentially a predictor of decline for perennial grasses and increase of some C_3 shrubs, however with only two of the eight sites showing that relationship, there is a need for more data (Munson *et al.* 2011a). Either indirectly through competitor decline or through actual benefits from lack of sensitivity to temperature, *E. viridis,* and possibly other C_3 shrubs, may be positively influenced by rising temperatures. While studies have looked at the increase or decrease of species densities due to changing climate variables, fewer studies have considered leaf-level sensitivities as indicators of those changes.

We sought to test if patterns of gas exchange and the sensitivity of photosynthesis to temperature and CO_2 may be related to patterns of C_3 shrub expansion and reductions in C_3 and C_4 grasses in the southwestern U.S. To test this, we investigated leaf-level ecophysiological variation and response curves among common shrub, forb, and grass species in perennial grassland ecosystems on the Colorado Plateau. By investigating biophysical and biochemical trait variations in species, we are attempting to understand the mechanisms underlying why some species respond positively to climate change and other do not. The three objectives of this research are to: 1) Use seasonal gas exchange measurements of photosynthetic CO_2 uptake and climate analyses to identify varying photosynthetic rates throughout the year and seasonal maxima; 2) Use temperature and CO_2 response curves to identify differences in biochemical and biophysical limitations among plant species; and 3) Use these biochemical and biophysical traits to group species based on similarities and compare whether increasing and decreasing species respond similarly to changing abiotic conditions.

Methods

Site Description

This study took place on the Colorado Plateau, just outside the Needles District of Canyonlands National Park (Figure 1). Measurements were taken at the USGS Extreme Drought in Grassland Experiment (EDGE) site in the vicinity of other related research (Munson *et al.* 2011a; Hoover *et al.* 2017). The site was chosen to maintain consistency across several studies investigating changes in plant species composition in the landscape. The site is categorized as a low elevation, deep, sandy soil perennial grassland dominated by *Coleogyne ramosissima* (Schwinning et al. 2008). Common species sampled at the site include both native and non-

native grass, forb, and shrub species in four plant functional types (C_3 grasses, C_4 grasses, C_3 forbs and C_3 shrubs) (see Table 1). The species we measured included seven forbs, four shrubs, and four grasses. We had 12 C_3 species and three C_4 species. Among our species, there were six annual and nine perennial species. 15-year monthly averages in temperature at our site showed yearly variation ranging between 4° and 36° C over the course of the year with July as the warmest month and January as the coolest. 2016 temperatures over the year followed the trends from the 15-year monthly averages except for warmer early summer temperatures in June and warmer early winter temperatures in October and November. In June, the driest month, precipitation averages 8 mm and in August to October averages are 30 to 33 mm (Figure 2). The trend for precipitation in 2016 varied from the trends of the 15-year monthly averages. Instead, June 2016 had 0.7 mm precipitation and 39 mm in July and August (see Figure 2) indicating warmer summer months, drier early summer months, and later precipitation in the year as climate models have predicted.

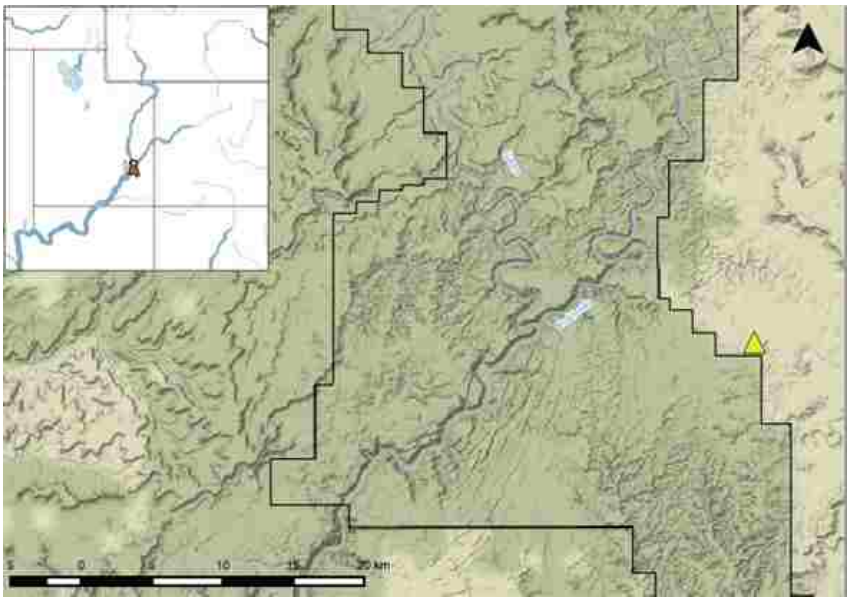

Figure 1
Map of the Canyonlands National Park area with our study site located just outside the Needles District. Measurements were taken at the USGS Extreme Drought in Grassland Experiment (EDGE) site (pictured as the yellow triangle) where other USGS studies (Munson et al. 2011 and Hoover et al. 2017) have taken place.

Study Design

To assess species-level differential sensitivities to rising temperature and CO_2 concentrations, we measured leaf-level gas exchange rates for 15 common species over the course of the year. Temperature response curves and A-C_i curves allow us to track changes in photosynthetic rates, biochemical parameters such as V_{cmax}, J_{max}, biophysical parameters such as stomatal regulation, and temperature optima as abiotic conditions change. Because plant sensitivity to changing abiotic conditions depends on seasonality, all measurements were taken six times over the course of a water year (December 2015, February, April, May, June, and September 2016). Sampling campaigns were chosen to represent different seasons with an extra two during the spring and summer months when plants are most active. Leaf-gas exchange measurements were taken using a LI-6400XT (LI-COR Inc., Lincoln, NE, USA) portable photosynthesis system with a standard leaf chamber and a fluorometer head for a consistent light source. Plants were sampled during the hours of 1000 and 1500 MDT over two days for each sampling campaign. Sampled individuals from the landscape were randomly chosen each time by setting up a transect, randomly generating a number, walking that transect, and sampling the closest individual. Individuals were sampled with a southern exposure to ensure full sunlight and plant activity before taking our measurements. We selected the youngest full expanded leaves to allow for a consistent leaf choice across our samples and branches, leaves or stems were chosen that were representative of the whole plant status. We sampled during days that had no precipitation and minimal variability in meteorological conditions across sampling time.

Table 1 Species measured in the study
Common Colorado Plateau species in our study area and their accompanying life form, photosynthetic pathway, and duration. Photosynthetic rates, temperature response curves, and A-Ci response curves were measured for each of these species throughout the year when they were photosynthetically active.

Common Name	Scientific Name	Lifeform	Pathway	Duration
Indian Rice Grass	*Achnatherum hymenoides*	Grass	C3	Perennial
Mat Amaranth	*Amaranthus blitoides*	Forb	C3	Annual
Crescent Milkvetch	*Astragalus amphioxys*	Forb	C3	Annual
Blue Grama	*Bouteloua gracilis*	Grass	C4	Perennial
Lambsquarters	*Chenopodium album*	Forb	C3	Annual
Rabbitbrush	*Chrysothamnus viscidiflorus*	Shrub	C3	Perennial
Blackbrush	*Coleogyne ramosissima*	Shrub	C3	Perennial
Mormon Tea	*Ephedra viridis*	Shrub	C3	Perennial
Bottlebrush	*Eriogonum inflatum*	Forb	C3	Perennial
Needle and Thread	*Hesperostipa comata*	Grass	C3	Perennial
Flatspine Stickseed	*Lappula occidentalis*	Forb	C3	Annual
Common Pepperweed	*Lepidium densiflorum var. ramosum*	Forb	C3	Annual
James' Galleta	*Pleuraphis jamesii*	Grass	C4	Perennial
Scarlet Globemallow	*Sphaeralcea coccinea*	Forb	C3	Perennial
Streptanthella Mustard	*Streptanthella longirostris*	Forb	C3	Annual

Climate Data

Climate data were collected from two sources to combine short- and long-term climate data. Short-term, site-specific data were measured from an on-site, USGS-managed weather station (EDGE_MET) located near the entrance to the Needles District of Canyonlands National Park on the Colorado Plateau (38.19130°, -109.746206°). Relative humidity and temperature measurements were recorded using Campbell Scientific CS215 probe. Precipitation was recorded using the Texas Electronic TE525MM rain gage. Soil moisture was measured using 30 cm water content reflectometer probes (CS650, Campbell Scientific, Logan, UT, USA) inserted horizontally at three depths: shallow (10 cm), intermediate (20 cm), and deep (40 cm). Long-term temperature and precipitation data were taken from the Climate Analyzer site using

National Weather Service data (COOP data, climateanalyzer.org) for the Needles District Visitor's Center weather station (Station ID: 421168) located across from the Visitor's Center just within park boundaries (38.167°, -109.759°). These data were used because they contained daily measurements for precipitation, maximum temperature, and minimum temperature for different sites in Canyonlands since 1965. Weather stations are 1.62 km (1 mile) apart.

Photosynthetic Gas Exchange Measurements

Leaf-level Photosynthesis Point Measurements

Leaf-level photosynthesis measurements were taken using the AutoProgram feature of the LI-6400XT machine set to sample at 5-s intervals for 2-6 minutes (depending on stability) with the following settings: light intensity was maintained at 2000 μmol m^{-2} s^{-1}, CO_2 concentration was at 400 μmol m^{-2} s^{-1}, and temperature and relative humidity were at ambient levels. Photosynthesis was calculated for each leaf by using an AutoGoldy script objective selection algorithm to choose a 30-second period where variability and slope were minimized. This reduced the likelihood of human error when choosing a stable time to stop the measurement. We measured species that were present and photosynthetically active at our site. Each measurement campaign, we took 15-20 point measurements for each species.

Given the unique plant structure of each species, we standardized the measurement location for placing the gas exchange between the fourth and fifth node on branches of *E. viridis*, 15 cm from the top of a straight branch of *C. ramosissima*, and on the middle of the leaf of the youngest fully emerged leaf for the grasses. For samples that did not cover the area of the LI-6400XT cuvette head, we clipped samples and measured surface area using ImageJ (IMAGEJ 1.48v, National Institutes of Health, Bethesda, MD, USA) and recalculated leaf area values on

the LI-6400XT machine.

A-C_i Response Curves

The A-C_i response curves were measured using the AutoProgram feature of the LI-6400XT machine. The same light intensity, humidity, and temperature settings used in the point measurements were used for the A-C_i curves. CO_2 levels were set to change from 400, 300, 200, 100, 50, 400, 600, and 800 ppm. The time spent at each step depended on the machine's internal stability. For each sampling campaign, we measured five individual plant's A-C_i response curves per species. A-C_i response curves were graphed and the carboxylation efficiency of the ribulose-1,5-biphosphate carboxylase/oxygenase (Rubisco) enzyme (J_{max}), the rate of electrons supplied by the electron transport chain (V_{cmax}), mesophyll conductance (g_m), and the ratio between the two (J/V_{cmax}) were calculated using protocol from Ethier and Livingston (2004). A-C_i curves that were included had R^2 values above 0.90. There were 1-3 curves per measurement campaign that we excluded from the analysis because of low R^2 values. Low R^2 values were due to sampling errors in the field such as batteries dying mid-measurement and insufficient time for stabilization before moving to the next step in the AutoProgram.

Temperature Response Curves

Temperature response curves settings were manually created using the AutoProgram feature of the LI-6400XT machine. Measurements were taken during the same time of day (1000 and 1500 MDT) but the starting temperature of the response curve varied according to the ambient temperature at the time the measurements was taken. This is due to cooling and heating abilities of the Li-COR. The machine can only hypothetically change the internal temperature

around +/- 6º C degrees (https://www.licor.com/env/products/photosynthesis/LI-6400XT/specs.html), but in practice, cooling the machine had a much smaller range (about 2º C). So the starting temperature for the temperature response curves was 2º C less than ambient temperature when measurements were taken. For winter months, temperature response curves began at around 12° C to 17° C for leaf temperatures. During the summer months, temperatures varied from 24° C to 30° C. Each step in the AutoProgram increased the temperature by 2° C and the time at each stage was controlled by internal stability measurements.

Statistical analyses

To determine whether measured gas exchange parameters (A, V_{cmax}, J_{max}, J/V_{cmax}, g_m, WUE) varied over the course of the year and across different species, we ran an ANOVA (aov) to examine responses of A, V_{cmax}, J_{max}, and $J/V_{cmax,}$ g_m, and WUE against our fixed effects (season, species, photosynthetic pathway (C_3, C_4), duration (annual, perennial), and lifeform (shrub, grass, forb)). We did not do a repeated measures ANOVA because for each sampling campaign, we selected new individuals to measure. We used season as an interaction term so we could compare the ecophysiological parameters as a factor of species and season (A ~ Species * Season). Data met the assumptions of normality so they were not transformed. When we checked for multicollinearity, we found that season and precipitation were strongly correlated. Season carried more weight in the analyses, so we opted to include season instead of precipitation. Pairwise comparisons were performed using t-tests with pooled standard deviations and a Bonferroni correction. For temperature response, we ran a linear regression model between temperature and photosynthesis for all the species taken together and for species individually over the sampled months. The models were graphed in R and curves were fitted using locally

weighted scatterplot smoothing (LOESS smoothing). To determine if all species had the same shape of temperature response, we used the Regression Wizard tool in Dynamic Curve Fitting model in Sigma Plot (Sigma Plot 10) to model temperature response over different curves. The final analyses we ran was a Discriminant Analysis of Principle Components (DAPC) weighted our measured variables (V_{cmax}, J_{max}, and $J/V_{cmax,}$ g_m, WUE, volumetric water content, season, functional type, duration, and lifeform) according to their importance and clustered species together according to the similarity of their responses. These variables were used to construct linear combinations of the original variables which have the largest between-group variance and the smallest-within group variance. We created six dimensions based on ten measured parameters. We retained eleven principal components, six clusters, and six discriminant functions. Based on the similarity of parameters, species were oriented on two axes for the DAPC to show clusters. The final step was to run model selection to determine the most influential parameters behind photosynthesis measurements and what combination best fit our data. We used the same parameters listed above for the DAPC with photosynthetic rate as the dependent variable. We used the Akaike's Information Criterion (AICc) to measure the relative quality of our model. The best model, or the best competing models, were selected based on the smallest AIC value and the total weight of the model (AICcWt). All statistical analyses were carried out using the statistical computing package R (R Core Team, 2013) with $P = 0.05$ as the critical level of significance.

Results

We sought to understand if patterns of gas exchange and the sensitivity of photosynthetic rate to temperature and CO_2 can identify physiological characteristics of species that are

increasing or decreasing in the southwestern U.S. To test this, we used leaf-level gas exchange measurements taken throughout the year in addition to temperature response curves and A-C_i response curves to show how sensitivity to changing abiotic conditions varied across species.

Our research finds three potential reasons for the increase of C_3 shrubs on the Colorado Plateau: 1) Evergreen C_3 shrubs (*E. viridis* and *C. ramosissima*) were functionally the same and were able to be photosynthetically active over the winter months when temperature and available moisture requirements were met (Figure 3), 2) Both C_3 and C_4 grass species were physiologically the same and did not separate out by photosynthetic pathway with different temperature and CO_2 conditions and 3) Shrubs have cooler temperature optima and a wider range and temperature optima than grass species giving them an advantage in cooler spring months and with more temperature variation (Table 3).

Precipitation and Temperature Measurements

Recorded precipitation and temperature measurements over the 2016 months resembled what we expected to see under climate change projections. The 2016 differences, while not extreme, showed an overall increase in summer and winter temperatures, more late summer precipitation and less winter precipitation than decadal averages (Figure 2). Compared to the fifteen-year averages, 2016 had warmer June temperatures (+3.2° C) with a 91% decrease in precipitation from 8 mm to 0.7 mm (Figure 2). From October to December, temperatures were 2.17° C, 1.99° C, and1.04° C higher in 2016 respectively. January and February were cooler in 2016 than the 15-year averages by 1.51° C and 0.53° C. February, April, May, July had 20-92% more precipitation than the 15-year averages. September to January had reduced precipitation 32-80% of previous decadal averages.

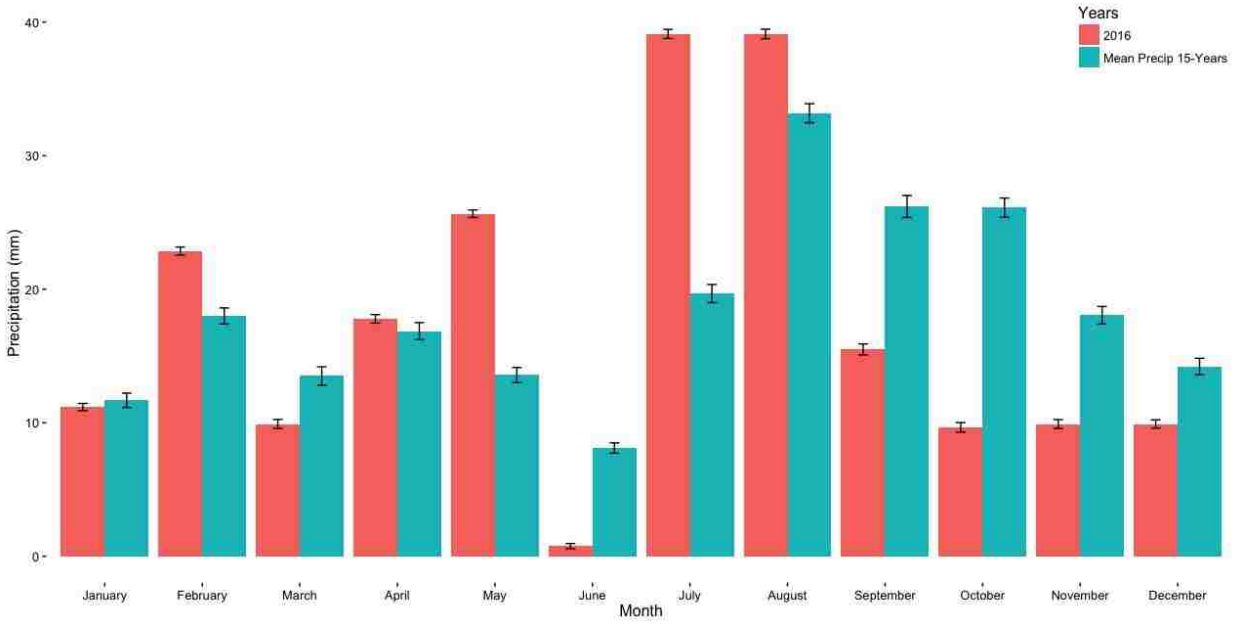

Figure 2 15-year average precipitation and monthly precipitation values graphed
Monthly precipitation values (mm) for 2016 graphed with the 15-year averages. Recorded precipitation measurements over the 2016 months resembled what we expected to see under climate change projections: more summer and less winter precipitation. It is important to note the variation in precipitation from June when there was hardly any rainfall and then in July and August when there was significantly more precipitation than the decadal averages.

Seasonal Gas Exchange Measurements

The three C_3 shrubs in our experiment were able to maintain photosynthetic activity over the winter months, a trait that is likely to confer a benefit over non-evergreen species (Figure 3 and Supplemental Table 1). Between our three common C_3 shrub species, *E. viridis*, *C. ramosissima*, and *C. viscidiflorus*, there were significant differences in winter photosynthetic rates when we ran the ANOVA (photosynthesis ~ species, p=0.0256, F value=3.725). In both December and February, *E. viridis* had the highest photosynthetic rates (Figure 3). The results of the pairwise comparison between species over winter months showed that *E. viridis* and *C. ramossisima* did not vary significantly in photosynthetic rates over winter (p=0.145) but

comparisons between *E. viridis* and *C. viscidiflorus* and *C. ramossisima* and *C. viscidiflorus* were significantly different ($p = 0.004$ and $p > 0.001$).

Overall, seasonality had the largest influence over peak photosynthetic rates (ANOVA, $p < 0.001$, F value=11.86). The only months that were not significantly different from each other in terms of species peak photosynthetic rates were fall and winter (pairwise comparison, $p=0.19$). The ANOVA interaction between season and species showed that within seasons, species photosynthetic rates significantly differed from each other ($p = 0.003$, F value=2.95). Over the course of the year, C_3 shrubs did not reach peak photosynthetic rates as high as forbs and grass species but they were able to maintain more consistent peak photosynthetic rates over the course of the year (Figure 3). This is especially pronounced for the C_3 species, *E. viridis*, which has an average photosynthetic rate of 11.43 µmol m^{-2} s^{-1} in April, 18.42 µmol m^{-2} s^{-1} in May and 16.62 µmol m^{-2} s^{-1} in June. The C_4 grass species, *Pleuraphis jamesii*, has a photosynthetic rate of 24.16 µmol m^{-2} s^{-1} in April, 29.57 µmol m^{-2} s^{-1} in May, and then drops off dramatically to 11.04 µmol m^{-2} s^{-1} in June (see Supplemental Table 1). Two shrub species, *E. viridis and C. viscidiflorus*, had among the highest measured photosynthetic rates in June (along with C_3 forb,

C. album), and *E. virdis* has the highest measured photosynthetic rate in September, December, and February.

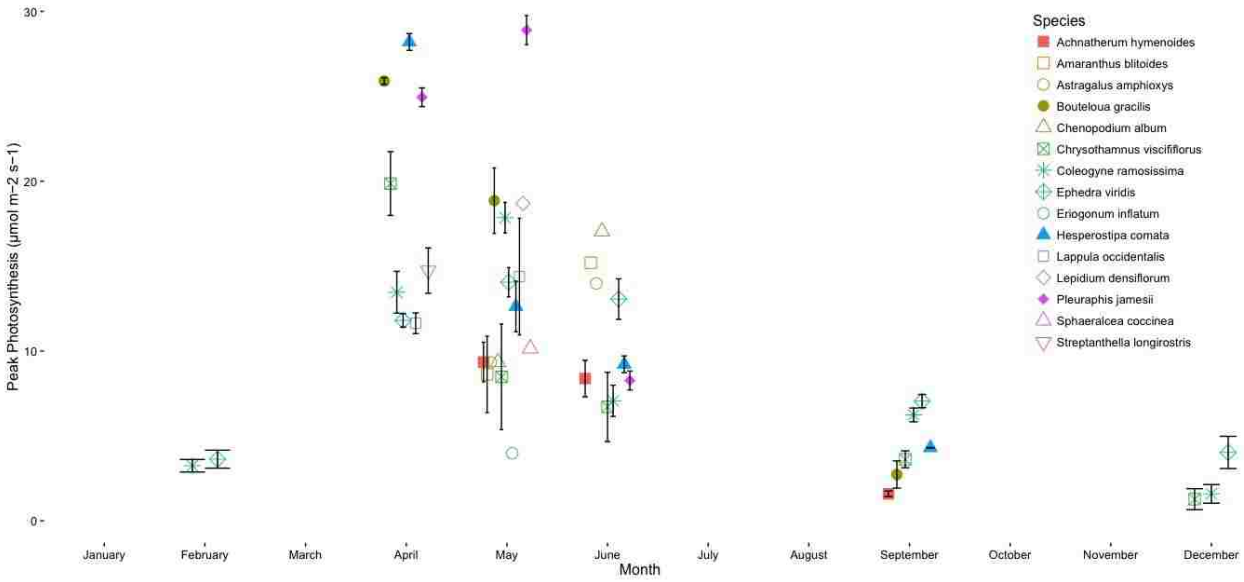

Figure 3 Point photosynthetic measurements
Leaf-level seasonal gas exchange measurements (µmol m^{-2} s^{-1}) for the 15 measured species. Grass species are identifiable by their filled in shapes, shrubs have lines through their shapes, and forbs are open-filled shapes. Shrub species have high rates of photosynthesis in April, May, and June (10-21 µmol m^{-2} s^{-1}) and slightly reduced rates throughout the rest of the year (2-7 µmol m^{-2} s^{-1}). Grass species have the highest rates of photosynthesis during spring and summer (17-30 µmol m^{-2} s^{-1}) which quickly drop off in September (3-7 µmol m^{-2} s^{-1}) and are not active in winter. Shrubs have a more consistent photosynthetic rate throughout the entire year which means fall and winter months they are still able to maintain activity when other species are not.

Temperature Response Curves and Optima

We found that, as expected, temperature influenced peak photosynthesis rates (linear regression, p=0.021, t value=-2.34) as well as identified differences among species over temperature response curves (linear regression with photosynthetic rate ~ temperature + species, p <0.001, t value=-8.89). The results from the linear regression for photosynthesis regressed by temperature and its interaction with species found that *E. viridis* is especially sensitive to increasing temperature (p=0.008, t-value=2.662). One C_3 grass, *Achnatherum hymenoides*, and the C_4 grass, *B. gracilis*, were also statistically sensitive to rising temperatures (p=0.044, t-

value= 2.017 and p=0.014, t-value=2.45). For all three species, increasing temperature led to an overall increase in photosynthetic rate (regression coefficients for *E. viridis* = 4.79, *A. hymenoides* = 5.54, *B. gracilis* = 4.80). This is consistent with the overall increase of species photosynthetic rate to rising temperature (p>0.001). Grass species have a slight decline (slope = -0.294), and shrubs and forbs have a slight increase (slopes = 0.471 and 0.117 respectively).

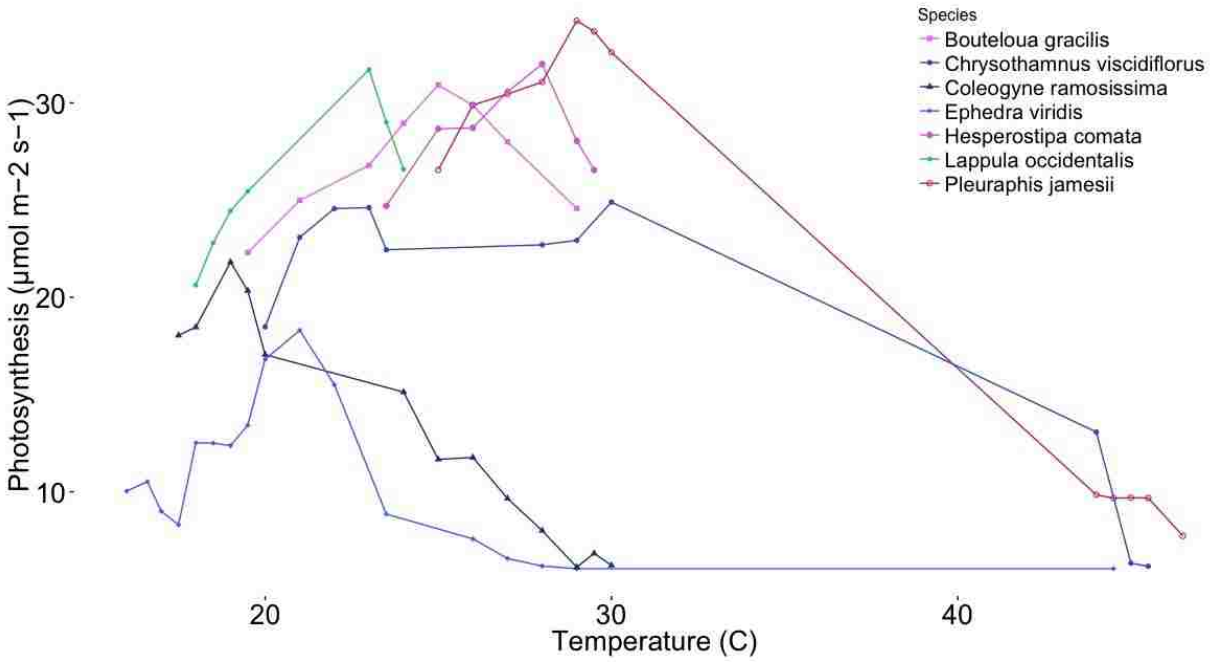

Figure 4 Temperature Response Curves
Temperature response curves for spring (April and May) 2016. C_3 and C_4 grasses species (graphed in shades of pink) had the highest photosynthetic rates and temperature optima, followed by forbs (green), and then shrubs (blue). While grass species had higher rates of photosynthesis, they also had a steeper incline to the peak and decline after the peak and a narrower curve, showing less generalized temperature optima.

For all species, the temperature response curves were sigmoidal with an increase in photosynthetic rate with warmer temperatures until a peak was reached, and then a decline after the peak (Figure 5). For *E. viridis* and *C. viscidiflorus*, the sigmoidal response curves had two peaks instead of one. In both cases, the first peak was lower, there was a period of acclimation, then a small drop, followed by an increase in photosynthetic rate until the second peak. The C_3 and C_4 grass species had higher peaks in photosynthetic rate and warmer temperature optima

(temperature at the highest photosynthetic rate) showing increased activity over warm conditions. C_3 shrub species reached a peak photosynthetic rate at 19-23° C. C_3 forb species reached a peak photosynthetic rate at 23° C. C_3 grass species reached a peak photosynthetic rate at 28° C. C_4 grass species reached 25-29° C (Table 2). While grass species had higher rates of photosynthesis, they also had a steeper incline to the peak and decline after the peak and a narrower curve, showing less generalized temperature optima (See Table 3). Although the peaks for shrubs are lower than for grasses, there is a wider range of temperatures where shrubs are photosynthesizing at, or near, their temperature optima.

Table 2 Species Spring maximum photosynthetic rate and optimum temperatures
Species max photosynthetic rate (μmol m^{-2} s^{-1}) and temperature optima (determined by peak photosynthetic range in the temperature response curves for each species and functional group) over spring months (April and May). C_3 and C_4 grass species had higher peaks in photosynthetic rate and warmer temperature optima showing increased activity over warm conditions. C_3 shrub species reached a peak photosynthetic rate at 19-23° C. C_3 forb species reached a peak photosynthetic rate at 23° C. C_3 grass species reached a peak photosynthetic rate at 28° C. C_4 grass species reached 25-29° C.

Species	Form	Pathway	Max Photosynthesis (μmol m^{-2} s^{-1})	Optimal ° C
Ephedra viridis	Shrub	C_3	18.3	21
Coleogyne ramosissima	Shrub	C_3	21.81	19
Chrysothamnus viscidiflorus	Shrub	C_3	24.61	23
Lappula occidentalis	Forb	C_3	31.71	23
Sphaeralcea coccinea	Forb	C_3	36.71	23.5
Hesperostipa comata	Grass	C_3	31.99	28
Bouteloua gracilis	Grass	C_4	30.91	25
Pleuraphis jamesii	Grass	C_4	34.22	29

Over the winter months (February and December), C_3 shrubs had a net positive photosynthesis rate starting at 16° C to 19° C. In 2016, we experienced a total of 18 winter days when peak daily temperatures were high enough for net positive photosynthetic activity in shrubs (Figure 4). We found that the number of days with shrub temperature optima over the winter months statistically and linearly increased over the past fifteen years ($p=0.003$, t value =3.069)

even though overall winter temperatures slightly cooled. We compared spring and winter precipitation and temperatures values because these are two important seasons for growth in the species we measured. Spring is when all of our species were most photosynthetically active. Winter represents the time when shrubs are active while grasses have senesced.

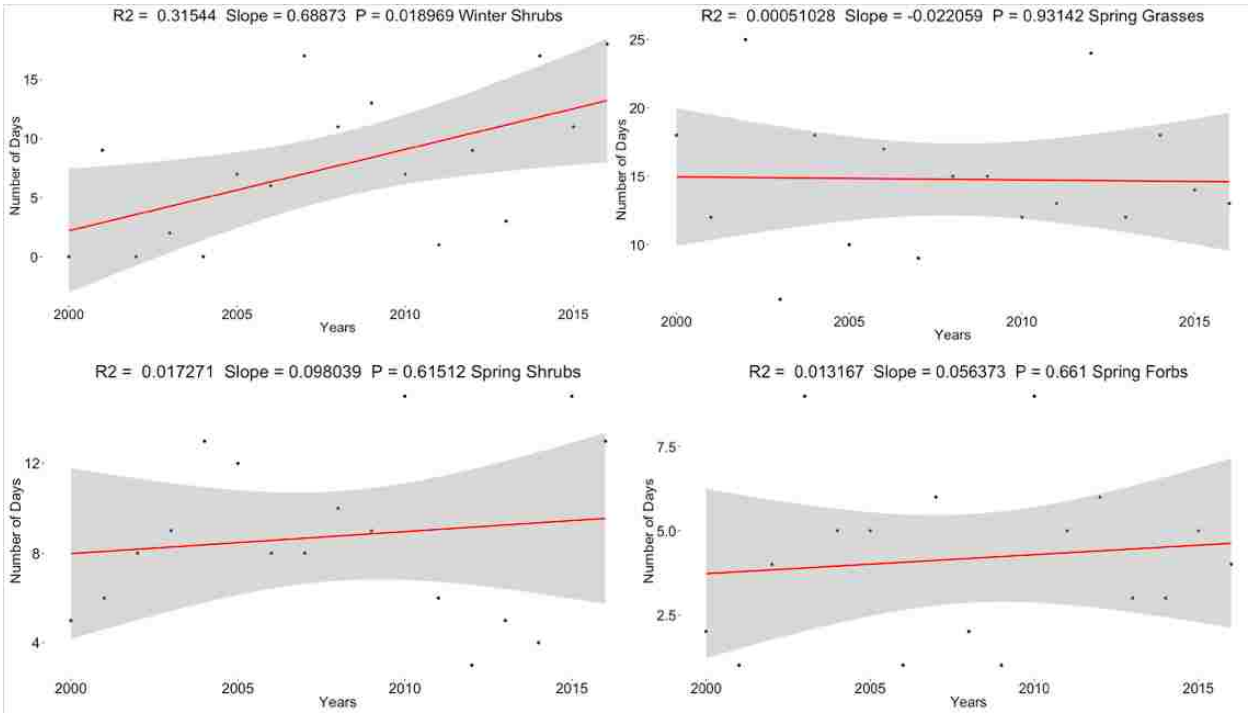

Figure 5 Temperature optima days over the past 15 years
Number of days with optimal temperatures for shrubs, grasses, and forbs over winter and spring months. The largest observed change occurred over winter months as the number of photosynthetically active days for shrubs increased ($p=0.01$, slope $=0.68$). In the spring, there was a slight increase in number of optimum days for shrubs and forbs and a decrease for grasses but not statistically significant.

A-C_i Response Curves

The graphed A-C_i response curves show two groups that respond to increasing CO_2 differently: CO_2 responsive species with very steep A-C_i curves showing fast response in A to increasing CO_2, and CO_2 conservative species, with slower responses and more conservative slopes (Figure 5). The C_3 grass and forb species are grouped together as CO_2 responsive, and the C_3 shrub species are grouped together as CO_2 conservative. The shrubs here show a marked

difference in slope, characterized by the biochemical parameter, V_{cmax}, and a lower elevation, characterized by the parameter J_{max}. From the ANOVA results, we can see that with all our measured biotic and abiotic factors included, species ($p<0.001$), season ($p<0.001$), and temperature ($p=0.004$) are the most influential in determining peak photosynthesis. In our study, V_{cmax} and J/V_{cmax} were influenced the most by photosynthetic pathway ($p=0.00826$, F-value=7.816, $p=0.00426$, F-value=9.31). J_{max} was influenced more by the abiotic conditions season ($p=0.0036$, F-value=5.453) and differences between species ($p=0.0279$, F-value=2.48). The model selection confirms that photosynthetic pathway describes almost all of the variation for V_{cmax} (AICcWt: 0.97) and precipitation and photosynthetic pathway can best describe J_{max} (AICcWt =0.96). In addition, species varied in their V_{cmax} values ($p<0.001$, F value=4.04) and the main differences between C_3 plants was with the shrub species, *C. viscidiflorous* and *C. ramosissima* ($p=0.00884$) and *E. viridis* ($p=0.0032$), the CO_2 conservative species.

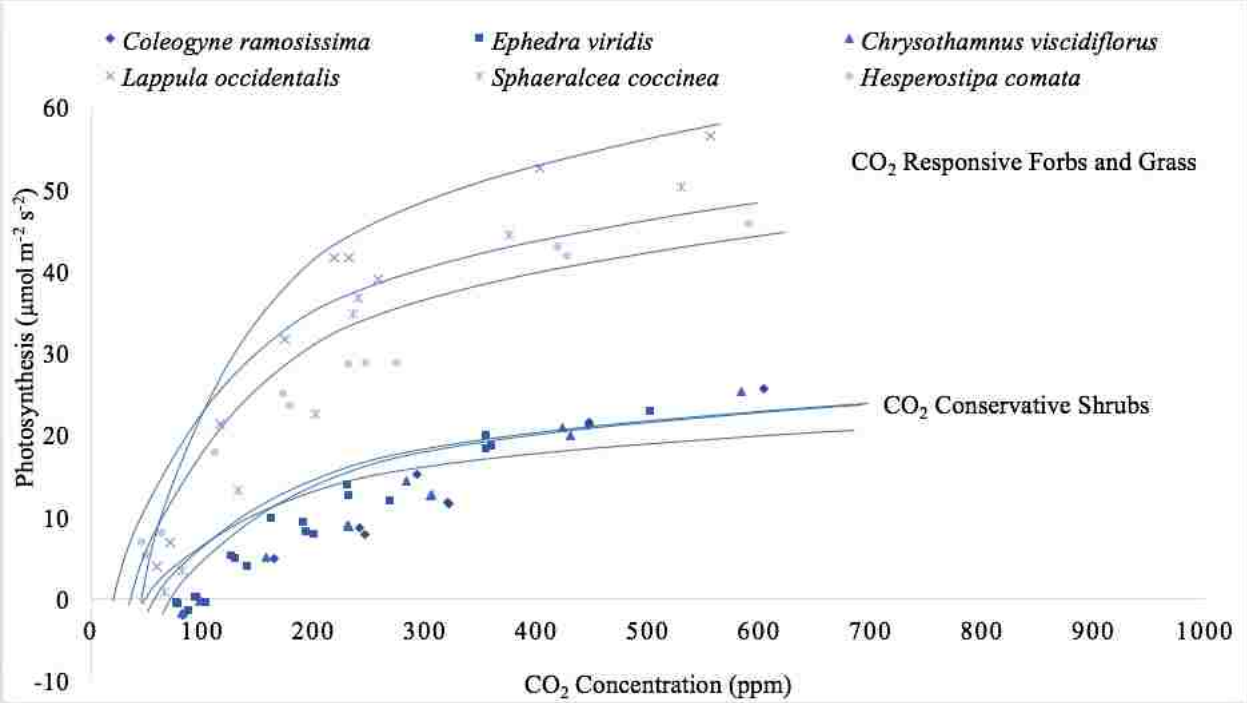

Figure 6 A-Ci curves
A-Ci response curves for C_3 grass, shrub, and forb species. A-C_i curves model photosynthetic CO_2 uptake rate (A) over changes in in intercellular CO_2 (c_i). Species with steep slopes (high V_{cmax}) and high elevations (high J_{max}) represent CO_2 responsive forb and grass species that are highly active with increases in CO_2. Species with gradual slopes and elevations we call CO_2 conservative species that do not respond as quickly to increases in CO_2

Grouping Species by General Strategies for Success

Photosynthetic pathway differences lead to the most discernable differences in photosynthetic rate between species ($p < 0.001$, F value = 14.08) followed by lifeform (grass vs. shrub vs. forb) ($p < 0.001$, F value = 4.212) (See Table 4). Overall grasses had the highest mean photosynthetic rate (regression coefficient = 12.57), followed closely by forbs (regression coefficient = 12.40), with shrubs further behind (regression coefficient = 8.20). In the pairwise comparison using t-tests, grasses and forbs did not significantly vary but forbs and shrubs ($p = 0.043$) and grasses and shrubs did ($p < 0.001$). C_4 photosynthetic pathway had higher rates of photosynthesis (regression coefficient = 15.33) compared to C_3 species (regression coefficient = 10.05).

Table 3 ANOVA results
ANOVA results for photosynthetic rate regressed by species, lifeform, photosynthetic pathway, month and interactions between independent variables (panel 1). HSD test for photosynthesis by month. Mean square error=29.43. The letters represent grouping. The same letters represent months that are not statistically different from each other.

Test	R Code	Df	F value	Pr (>F)
aov	Photo ~ Species	14	1.769	0.0495
aov	Photo ~ Lifeform	2	4.212	0.0166
aov	Photo ~ Pathway	1	14.08	<0.001
aov	Photo ~ Month	5	19.51	<0.001
aov	Photo ~ Species * Season	15	4.465	<0.001
aov	Photo ~ Species * Month	22	9.96	<0.001
aov	WinterPhoto ~ Species	2	3.725	0.025

Groups	Treatments	Means
a	May	14.52
a	April	14.32
b	June	9.78
c	September	4.47
c	December	1.78
c	February	1.19

In the Discriminant Analysis of Principal Components (DAPC), our species divided into six clusters. For the first axis, which accounts for 58% of the variation in photosynthetic rate, the key loading is based on photosynthetic pathway and mesophyll conductance (g_m), and the second axis loads primarily by light respiration (R_d), lifeform, J/V_{cmax}, and photosynthetic pathway (Figure 7 and 8). The six clusters largely separate into lifeform groupings: 1) *Sphaeralcea coccinea* and *Gutierrezia microcephala* (C_3 forb and shrub); 2) *Chrysothamnus viscidiflorus* (C_3 shrub); 3) *E. viridis* and *C. ramosissima* (C_3 shrubs); 4) *Bouteloua gracilis* (C_4 grass); 5) *Lappula occidentalis* and *Streptanthella longirostris* (C_3 forbs); and 6) *Pleuraphis jamesii* and *Hesperostipa comata* (C_4 and C_3 grass). While most of the grouping represented functional groups, evergreen, increasing woody shrubs, *C. ramosissima* and *E. viridis* grouped more closely to the C_3 and C_4 grass species and further from the other shrub and forb species.

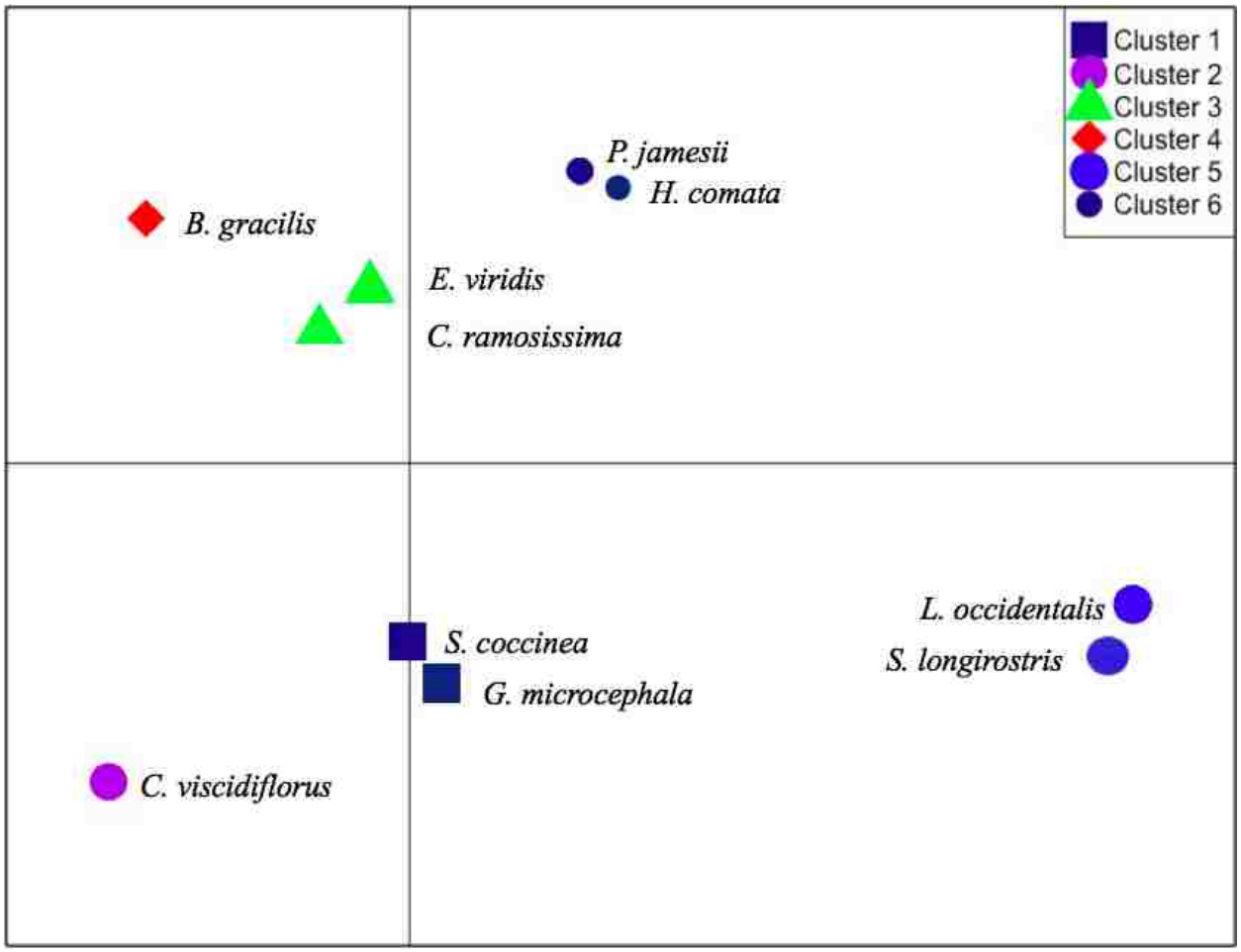

Figure 7 Clustering of species by similar traits
Discriminant Analysis of Principle Components (DAPC) showing the clustering of groups of species. Clusters represent combinations of the ecophysiological variables which have the largest between-group variance and the smallest-within group variance. Cluster 3 includes increasing species (*E. viridis* and *C. ramosissima*), clusters 4 and 6 are decreasing grass species (*B. gracilis*, *P. jamesii*, and *H. comata*) and the other groups have no known changes.

From the PCA loadings of these variables, the strongest parameters defining the axes are biophysical (mesophyll conductance and light respiration), biochemical (photosynthetic pathway and J/V_{cmax}), and structural (photosynthetic pathway and lifeform) (Figure 8). In the clusters defined by the DAPC, increasing species, *E. viridis and C. ramosissima* are found grouped together and decreasing species, *B. gracilis*, *P. jamesii*, *H. comata*) comprise two groups. The forbs are clustered toward the bottom of the chart together showing similar values of the

ecophysiological parameters. Interestingly, both the increasing species cluster and the decreasing species clusters spatially arrange near each other in the upper half of the figure.

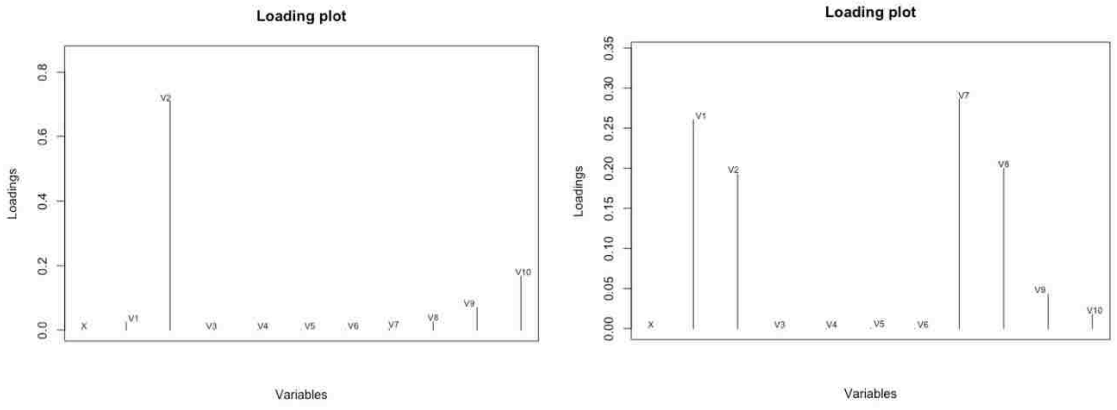

Figure 8 Important variables in clustering
Loading plots for both DAPC axes showing important variables in clustering species. For axis one, photosynthetic pathway is the most important variable (V2), followed by mesophyll conductance (V10). For axis two, species were grouped into clustered based on light respiration (V7), J/V_{cmax} (V8), lifeform (V1), and photosynthetic pathway (V2).

Discussion

Anthropogenic climate change, driven by increases in atmospheric CO_2 is projected to cause rising temperature and shifts in plant community composition (Shaw *et al.* 1998; Sheffield and Wood 2008b, a; Christensen *et al.* 2007). Given that these abiotic changes will alter plant photosynthetic rates, we focused on leaf-level plant ecophysiology measurements to identify plant sensitivities to rising CO_2. In order to determine whether increasing species (C_3 shrubs) display similar sensitivities and patterns of gas exchange to temperature and CO_2, we took seasonal, leaf-level gas exchange measurements and measured temperature and CO_2 response curves. Overall we found that C_3 shrubs are able to maintain higher photosynthetic rates over spring and summer, are more physiologically active over the increasingly warmer winter months, and have wider range of temperature optima than grass species. Increasing atmospheric CO_2

concentrations, on the other hand, benefit responsive C_3 and C_4 grass species through an increase in photosynthetic activity.

Seasonal Gas Exchange Measurements

Our objective was to determine whether plants increasing on the Colorado Plateau displayed commonalities that might lead to their success in climate changing conditions. The biggest indication of their success, from the data we collected, is the increased activity over winter months. Not only we were able to find that shrubs are active over the winter months, but that their activity was not statistically different from fall months. This, combined with the fact that grasses are senesced during those months means that there is limited competition for shrubs during the winter.

While C_3 shrub species show a reduction in peak photosynthesis values over winter months, they consistently have positive net photosynthetic activity when temperature minimums are met (Figure 3). Our site experienced an overall cooler average temperature in 2016 compared to the 15-year averages but with twice as many warm days. These conditions are likely to benefit shrubs that are hardy enough to survive the cooler temperatures and also able to be photosynthetically active on days when minimum photosynthetic requirements are met. D'Odorico *et al.* (2010) found that woody plant encroachment is largely due to the warming of nighttime air in winter months in the Chihuahuan Desert. They predict that small warming can yield meaningful changes in shrub species. The authors suggest that the effect of changing air temperature on vegetation depends on whether plants experience drought during the winter months. Because of different annual distribution of precipitation and potential evapotranspiration between the Colorado Plateau and the Chihuahuan desert where the abovementioned study was

conducted, the warming of winter months could be more significant in more arid desert communities (D'Odorico *et al.* 2010).

Warmer winter temperatures were not spread out equally throughout the winter months. Daily temperature measurements show that there are increasing number of warm winter days at the end of October and carrying into the beginning of November. Warming during these months paired with late season precipitation, is likely to lead to increasing growth over these months. *E. viridis* could disproportionality benefit from these climatic changes because the species had the highest photosynthetic rate from June to February among the species we measured. Not only will evergreen shrubs be increasing during these months when they conditions are right and competition reduced, but *E. viridis* and *C. ramosissima*, both woody shrubs, are expected to perform better than other shrub species because of its slightly elevated photosynthetic rate.

E. viridis (Gymnospermae; Gnetales; Ephedraceae) has several traits that could explain its success. As an evergreen, woody shrub with dense clusters of erect green twigs, *E. virdis* is photosynthetically active year-round. As a shrub, it has deep, woody roots that may extend deep into the well, drained, sandy soils (Anderson 2001). It is found exclusively in the western United States around the arid Great Basin Region, Colorado, San Juan and Rio Grande drainages. While grazing has been shown to explain increases in shrub expansion in other studies (DeMalach *et al.* 2014), the 2011 Munson *et al.* study took place in long-term plots inside the boundaries of national parks and BLM lands, suggesting that grazing alone is unlikely to explain the increase in canopy cover of *E. viridis*. Legacy effects of grazing from prior to the 1960s and 70s could potentially play a role in community dynamics but further examination of that is needed.

The Munson *et al.* (2011) data showed increases in *E. viridis* corresponded to high summer temperatures in the previous year. While our results do not directly suggest that high

summer temperatures benefit *E. viridis* and other shrubs, it is possible that previous year hot summer temperatures also lead to warmer winters. Yoder and Nowak (1999) hypothesize that the growth of *E. viridis* may be affected by high temperatures because it receives much of its water from winter precipitation when temperatures are low. With increasing winter temperatures over the winter months, soil water availability could decline as shrub species tap into those resources for photosynthesis.

Temperature and CO_2 Response Curves

Temperature and CO_2 response curves did not consistently benefit one species or functional group. In the spring temperature response curves, C_3 shrub species had the lowest peak photosynthetic rate and the lowest temperature optima. In 2016, our site experienced lower spring temperatures that, if continued, could lead to increased activity for shrub and forb species.

This is likely due to the cooler spring temperatures which reach peak temperature ranges for shrubs and forbs which are slightly lower than grass temperature optima (Figure 4). This confers a competitive advantage for the species during this period because over the cooler winter months, they are still able to be active at similar rates to fall while their competitor species are senesced. Grasses have the advantage with increasingly warmer temperatures. Their temperature optima were consistently much higher than shrubs and forbs, with C_4 grasses at the highest. This is consistent with findings that the contrasting physiological responses of C_3 and C_4 plants to warming, is the main driver of observed patterns of plant assemblage structure (Duffy & Chown, 2016).

Grass species, through their responsiveness to increasing concentrations of atmospheric CO_2, are likely to benefit from rising atmospheric concentrations in our region. While grasses

and forbs benefited from the short term addition of CO_2, it does not necessarily mean they will maintain elevated photosynthetic rates with higher CO_2 concentrations over a longer period of time. Ainsworth *et al.* (2003) found a 43% higher rate of light-saturated leaf photosynthesis in grasses over 10 years in elevated CO_2 conditions. Other studies have found no difference in densities of plants grown in higher CO_2 conditions (Blumenthal *et al.* 2016). Entire research methodologies like the Free-Air Concentration Enrichment (FACE) exist to test whether the photosynthetic responses of species to increasing CO_2 in closed chamber experiments is what will actually happen in the field.

In terms of the biochemical and biophysical reactions of plants to increased CO_2, photosynthetic pathway was the most important indicator of V_{cmax} and $J/V_{cmax.}$ while J_{max} was influenced by precipitation and differences between species. This is consistent with findings that J/V_{cmax}, the ratio between the maximum rate of electron transport driving RuBP regeneration (J_{max}) and the in vivo maximum rate of RuBP carboxylation (V_{cmax}), has been shown to change from species to species depending on abiotic conditions (Onoda *et al.* 2004). The variation in J/V_{cmax} across seasons did not vary as much as it did between species (Onoda *et al.* 2004). This is demonstrated in the graphed A-C_i curves which show the CO_2 conservative species with a reduced slope and elevation of the curve. Curves like these that are less steep indicate a broad range of stomatal limitations. These limitations shape plants ability to capture carbon while avoiding water loss, a key requirement for survival in dryland ecosystems (Amthor 1995; Blumenthal *et al.* 2016). Elevated atmospheric CO_2 concentration stimulates forbs and grass species photosynthetic rates more than shrubs, reduces stomatal and mesophyll conductance, and inhibits plant respiration, as several studies have also found (Idso *et al.* 1993; Callaway *et al.* 1994; Gunderson and Wullschleger 1994; Jackson *et al.* 1994; Amthor 1995; Polley *et al.* 2013).

Grouping of General Strategies for Success

In the groupings from the Discriminant Analysis of Principal Components (DAPC), we found that functional trait differences contributed to increased or decreased sensitivity in the species we measured. Among those species, lifeform and photosynthetic pathway were the most important traits in determining peak photosynthetic rate. Other than that, there were several ecophysiological parameters that are able to separate species from each other: mesophyll conductance (g_m), light respiration (R_d), J/V_{cmax}. While the scope of our research does not attempt to explain why different species and functional groups respond variably to changing abiotic conditions, other research has come out on the issue. In high light conditions like ours, researchers have found that chloroplast CO_2 concentration (C_c) in C_4 leaves are 8-10 times higher than C_3 leaves, explaining why there is virtually no photorespiration in C_4 leaves (Yin & Struik 2009). Differences in J/V_{cmax} has been shown to indicate leaf nitrogen, phosphorus, and specific leaf area values (Walker *et al*. 2014). Walker *et al*. (2014) found that increasing leaf P substantially increased the sensitivity of V_{cmax} to leaf N (Walker *et al*. 2014). While dryland ecosystems are primarily limited by water availability, they are also known for the restrictions on plant growth and nutrient uptake that limiting available N and P creates (James *et al.* 2005; He *et al.* 2014). With climate changing precipitation regimes, availability of N and P could become more important during seasons with increasing rainfall.

Conclusions

It is unlikely that one factor alone can explain the increase in some species and the decreases in others in arid ecosystems. Our objective was to determine whether plants increasing on the Colorado Plateau displayed commonalities that might lead to their success in climate

changing conditions. The most significant indication of shrub success in our site was the increasing photosynthetic activity over the winter months. While photosynthesis rates over winter were not comparable to those in the spring, that time still represents limited competition between shrubs and senesced grass species, available resources from late season precipitation, and increasing warmer winter months. In climate changing conditions, warmer winter months in arid ecosystems might continue to benefit shrub species and have a disproportionately larger effect than increasing summer temperatures and atmospheric CO_2 concentrations.

References

Adler, P. B., and J. HilleRisLambers. 2008. The influence of climate and species composition on the population dynamics of ten prairie forbs. Ecology 89:3049-3060.

Ainsworth, E. A., P. A. Davey, G. J. Hymus, C. P. Osborne, A. Rogers, H. Blum, J. Nosberger, and S. P. Long. 2003. Is stimulation of leaf photosynthesis by elevated carbon dioxide concentration maintained in the long term? A test with Lolium perenne grown for 10 years at two nitrogen fertilization levels under Free Air CO(2) Enrichment (FACE). Plant Cell and Environment 26:705-714.

Algar, A. C., H. M. Kharouba, E. R. Young, and J. T. Kerr. 2009. Predicting the future of species diversity: macroecological theory, climate change, and direct tests of alternative forecasting methods. Ecography 32:22-33.

Amthor, J. S. 1995. Terrestrial higher-plant response to increasing atmospheric CO2 in relation to the global carbon cycle. Global Change Biology 1:243-274.

Anderson, Michelle D. 2001. Ephedra viridis. In: Fire Effects Information System, [Online]. U.S. Department of Agriculture, Forest Service, Rocky Mountain Research Station, Fire Sciences Laboratory (Producer). Available: http://www.fs.fed.us/database/feis/ [2017, August 8].

Apple, M. E., D. M. Olszyk, D. P. Ormrod, A. Lewis, D. Southworth, and D. T. Tingey. 2000. Morphology and stomatal function of Douglas fir needles exposed to climate chance: Elevated CO2 and temperature. International Journal of Plant Sciences 161:127-132.

Blumenthal, D. M., J. A. Kray, W. Ortmans, L. H. Ziska, and E. Pendall. 2016. Cheatgrass is favored by warming but not CO2 enrichment in a semi-arid grassland. Global Change Biology 22:3026-3038.

Bowes, G. 1993. FACING THE INEVITABLE - PLANTS AND INCREASING ATMOSPHERIC CO(2). Annual Review of Plant Physiology and Plant Molecular Biology 44:309-332.

Callaway, R. M., E. H. Delucia, E. M. Thomas, and W. H. Schlesinger. 1994. Compensatory responses of CO2 exchange and biomass allocation and their effects on the relative growth-rate of Ponderosa Pine in different CO2 and temperature regimes. Oecologia 98:159-166.

Christensen, J. H., T. R. Carter, M. Rummukainen, and G. Amanatidis. 2007. Evaluating the performance and utility of regional climate models: the PRUDENCE project. Climatic Change 81:1-6.

Cunniff, J., G. Jones, M. Charles, and C. P. Osborne. 2017. Yield responses of wild C-3 and C-4 crop progenitors to subambient CO2: a test for the role of CO2 limitation in the origin of agriculture. Global Change Biology 23:380-393.

D'Odorico, P., J. D. Fuentes, W. T. Pockman, S. L. Collins, Y. He, J. S. Medeiros, S. Dewekker, and M. E. Litvak. 2010. Positive feedback between microclimate and shrub encroachment in the northern Chihuahuan desert. Ecosphere 1.

Davies, S. J. 1998. Photosynthesis of nine pioneer Macaranga species from Borneo in relation to life history. Ecology 79:2292-2308.

Dawson, T. E., J. K. Ward, and J. R. Ehleringer. 2004. Temporal scaling of physiological responses from gas exchange to tree rings: a gender-specific study of Acer negundo (Boxelder) growing under different conditions. Functional Ecology 18:212-222.

DeMalach, N. Are semiarid shrubs resilient to drought and grazing? 2014. Differences and similarities among species and habitats in a long-term study. Journal of Arid Environments. 102:1-8.

Diffenbaugh, N. S., J. S. Pal, R. J. Trapp, and F. Giorgi. 2005. Fine-scale processes regulate the response of extreme events to global climate change. Proceedings of the National Academy of Sciences of the United States of America 102:15774-15778.

Drake, B. G., M. A. GonzalezMeler, and S. P. Long. 1997. More efficient plants: A consequence of rising atmospheric CO2? Annual Review of Plant Physiology and Plant Molecular Biology 48:609-639.

Duffy, G. A., and S. L. Chown. 2016. Urban warming favours C-4 plants in temperate European cities. Journal of Ecology 104:1618-1626.

Easterling, D. R., G. A. Meehl, C. Parmesan, S. A. Changnon, T. R. Karl, and L. O. Mearns. 2000. Climate extremes: Observations, modeling, and impacts. Science 289:2068-2074.

Fay, P. A., B. A. Newingham, H. W. Polley, J. A. Morgan, D. R. LeCain, R. S. Nowak, and S. D. Smith. 2015. Dominant plant taxa predict plant productivity responses to CO2 enrichment across precipitation and soil gradients. Aob Plants 7:10.

Ghouil, H., P. Montpied, D. Epron, M. Ksontini, B. Hanchi, and E. Dreyer. 2003. Thermal optima of photosynthetic functions and thermostability of photochemistry in cork oak seedlings. Tree Physiology 23:1031-1039.

Gunderson, C. A., and S. D. Wullschleger. 1994. Photosynthetic acclimation in trees to rising atmospheric CO2- A broader perspective Photosynthesis Research 39:369-388.

Herrick, J. D., and R. B. Thomas. 1999. Effects of CO2 enrichment on the photosynthetic light response of sun and shade leaves of canopy sweetgum trees (Liquidambar styraciflua) in a forest ecosystem. Tree Physiology 19:779-786.

Heskel, M.A. O.S. O'Sullivan, P.B. Reich, M.G. Tjoelker, L.K. Weerasinghe, A. Penillard, J.J.G. Egerton, D. Creek, K.J. Bloomfield, J. Xiang, F. Sinca, Z.R. Stangl, A. Martinez-de la Torre, K.L. Griffin, C. Huntingford, V. Hurry, P. Meir, M.H. Turnbull, O.K. Atkin. Convergence in the temperature response of leaf respiration across biomes and plant functional types. 2016. Proceedings of the National Academy of Sciences of the United States of America. 113:14:3832:3837

Hoover, D. L., M. C. Duniway, and J. Belnap. 2015. Pulse-drought atop press-drought: unexpected plant responses and implications for dryland ecosystems. Oecologia 179:1211-1221.

Hoover, D. L., A. K. Knapp, and M. D. Smith. 2014. Resistance and resilience of a grassland ecosystem to climate extremes. Ecology 95:2646-2656.

Hu, L. X., Z. L. Wang, and B. R. Huang. 2010. Diffusion limitations and metabolic factors associated with inhibition and recovery of photosynthesis from drought stress in a C-3 perennial grass species. Physiologia Plantarum 139:93-106.

Huxman, T. E., E. P. Hamerlynck, M. E. Loik, and S. D. Smith. 1998. Gas exchange and chlorophyll fluorescence responses of three south-western Yucca species to elevated CO2 and high temperature. Plant Cell and Environment 21:1275-1283.

Idso, S. B., B. A. Kimball, and D. L. Hendrix. 1993. Air-temperature modifies the size-enhancing effects of atmospheric CO2 enrichment on sour orange tree leaves. Environmental and Experimental Botany 33:293-299.

Jackson, R. B., O. E. Sala, C. B. Field, and H. A. Mooney. 1994. CO2 alters water-use, carbon gain, and yield for the dominant species in a natural grassland. Oecologia 98:257-262.

Jochum, G. M., K. W. Mudge, and R. B. Thomas. 2007. Elevated temperatures increase leaf senescence and root secondary metabolite concentrations in the understory herb Panax quinquefolius (Araliaceae). American Journal of Botany 94:819-826.

Jones, H. G. 1973. Moderate term water stresses and associated changes in some photosynthetic parameters in cotton. New Phytologist 72:1095-1105.

Karl, T. R. (Ed.). (2009). Global climate change impacts in the United States. Cambridge University Press.

Liang, J. Y., J. Y. Xia, L. L. Liu, and S. Q. Wan. 2013. Global patterns of the responses of leaf-level photosynthesis and respiration in terrestrial plants to experimental warming. Journal of Plant Ecology 6:437-447.

Lusk, C. H., and A. Del Pozo. 2002. Survival and growth of seedlings of 12 Chilean rainforest trees in two light environments: Gas exchange and biomass distribution correlates. Austral Ecology 27:173-182.

Lusk, C. H., I. Wright, and P. B. Reich. 2003. Photosynthetic differences contribute to competitive advantage of evergreen angiosperm trees over evergreen conifers in productive habitats. New Phytologist 160:329-336.

Momen, B., S. J. Behling, G. B. Lawrence, and J. H. Sullivan. 2015. Photosynthetic and Growth Response of Sugar Maple (Acer saccharum Marsh.) Mature Trees and Seedlings to Calcium, Magnesium, and Nitrogen Additions in the Catskill Mountains, NY, USA. Plos One 10:14.

Munson, S. M., J. Belnap, and G. S. Okin. 2011a. Responses of wind erosion to climate-induced vegetation changes on the Colorado Plateau. Proceedings of the National Academy of Sciences of the United States of America 108:3854-3859.

Munson, S. M., J. Belnap, C. D. Schelz, M. Moran, and T. W. Carolin. 2011b. On the brink of change: plant responses to climate on the Colorado Plateau. Ecosphere 2:15.

Niu, S. L., Z. X. Li, J. Y. Xia, Y. Han, M. Y. Wu, and S. Wan. 2008. Climatic warming changes plant photosynthesis and its temperature dependence in a temperate steppe of northern China. Environmental and Experimental Botany 63:91-101.

Onoda, Y., K. Hikosaka, and T. Hirose. 2005. Seasonal change in the balance between capacities of RuBP carboxylation and RuBP regeneration affects CO2 response of photosynthesis in Polygonum cuspidatum. Journal of Experimental Botany 56:755-763.

Pataki, D. E., R. Oren, and D. T. Tissue. 1998. Elevated carbon dioxide does not affect average canopy stomatal conductance of Pinus taeda L. Oecologia 117:47-52.

Pearcy, R.W. and Ehleringer, J. Comparative Ecophysiology of C-3 and C-4 Plants. 1984. Plant Cell and Environment. 7:1:1-13.

Polley, H. W., D. D. Briske, J. A. Morgan, K. Wolter, D. W. Bailey, and J. R. Brown. 2013. Climate Change and North American Rangelands: Trends, Projections, and Implications. Rangeland Ecology & Management 66:493-511.

R Core Team (2013). R: A language and environment for statistical computing. R Foundation for Statistical Computing, Vienna, Austria. ISBN 3-900051-07-0, URL *http://www.R-project.org/*

Romero, P., and P. Botia. 2006. Daily and seasonal patterns of leaf water relations and gas exchange of regulated deficit-irrigated almond trees under semiarid conditions. Environmental and Experimental Botany 56:158-173.

Sage, R. F., and R. Khoshravesh. 2016. Passive CO2 concentration in higher plants. Current Opinion in Plant Biology 31:58-65.

Schwinning, S., J. Belnap, D. R. Bowling, and J. R. Ehleringer. 2008. Sensitivity of the Colorado Plateau to Change: Climate, Ecosystems, and Society. Ecology and Society 13.

Shaw, G. E., R. L. Benner, W. Cantrell, and A. D. Clarke. 1998. The regulation of climate: A sulfate particle feedback loop involving deep convection - An editorial essay. Climatic Change 39:23-33.

Sheffield, J., and E. F. Wood. 2008a. Global trends and variability in soil moisture and drought characteristics, 1950-2000, from observation-driven Simulations of the terrestrial hydrologic cycle. Journal of Climate 21:432-458.

Sheffield, J., and E. F. Wood. 2008b. Projected changes in drought occurrence under future global warming from multi-model, multi-scenario, IPCC AR4 simulations. Climate Dynamics 31:79-105.

Sheppard, C. S., and M. C. Stanley. 2014. Does Elevated Temperature and Doubled CO2 Increase Growth of Three Potentially Invasive Plants? Invasive Plant Science and Management 7:237-246.

Sholtis, J. D., C. A. Gunderson, R. J. Norby, and D. T. Tissue. 2004. Persistent stimulation of photosynthesis by elevated CO2 in a sweetgum (Liquidambar styraciflua) forest stand. New Phytologist 162:343-354.

Sigut, L., P. Holisova, K. Klem, M. Sprtova, C. Calfapietra, M. V. Marek, V. Spunda, and O. Urban. 2015. Does long-term cultivation of saplings under elevated CO2 concentration influence their photosynthetic response to temperature? Annals of Botany 116:929-939.

Sobrado, M. A. 2000. Relation of water transport to leaf gas exchange properties in three mangrove species. Trees-Structure and Function 14:258-262.

Song, B., S. L. Niu, and S. Q. Wan. 2016. Precipitation regulates plant gas exchange and its long-term response to climate change in a temperate grassland. Journal of Plant Ecology 9:531-541.

Sun, D. F., R. Dawson, H. Li, R. Wei, and B. G. Li. 2007. A landscape connectivity index for assessing desertification: a case study of Minqin County, China. Landscape Ecology 22:531-543.

Tooth, I. M., and M. R. Leishman. 2014. Elevated carbon dioxide and fire reduce biomass of native grass species when grown in competition with invasive exotic grasses in a savanna experimental system. Biological Invasions 16:257-268.

Valerio, M., M. Tomecek, S. Lovelli, and L. Ziska. 2013. Assessing the impact of increasing carbon dioxide and temperature on crop-weed interactions for tomato and a C-3 and C-4 weed species. European Journal of Agronomy 50:60-65.

Walker, A.P, A.P. Beckerman, L.H. Gu, J. Katthe, L.A. Cernusak, T.F. Domingues, J.C. Scales, G. Wohlfahrt, S.D. Wullschleger, F.I. Woodward. 2014. Ecology and Evolution. 4:16:3218-3236.

Wand, S. J. E., G. F. Midgley, M. H. Jones, and P. S. Curtis. 1999. Responses of wild C4 and C3 grass (Poaceae) species to elevated atmospheric CO2 concentration: a meta-analytic test of current theories and perceptions. Global Change Biology 5:723-741.

Wang, D., S. A. Heckathorn, X. Z. Wang, and S. M. Philpott. 2012. A meta-analysis of plant physiological and growth responses to temperature and elevated CO2. Oecologia 169:1-13.

Wullschleger, S. D., C. A. Gunderson, P. J. Hanson, K. B. Wilson, and R. J. Norby. 2002. Sensitivity of stomatal and canopy conductance to elevated CO2 concentration - interacting variables and perspectives of scale. New Phytologist 153:485-496.

Xu, Z. Z., and G. S. Zhou. 2005. Effects of water stress and high nocturnal temperature on photosynthesis and nitrogen level of a perennial grass Leymus chinensis. Plant and Soil 269:131-139.

Yin, X and Struik, P.C. C-3 and C-4 photosynthesis models: An overview from the perspective of crop modelling. 2009. Njas-Wageningen Journal of Life Science. 57:1:27-38.

Ziska, L. H. 2001. Growth temperature can alter the temperature dependent stimulation of photosynthesis by elevated carbon dioxide in Albutilon theophrasti. Physiologia Plantarum 111:322-328.

Chapter 2:

Using Very High Resolution (VHR) satellite Imagery to Create an Accurate, Species-level Baseline Map in Canyon Terrain

Abstract

Accurate species distribution mapping is crucial for assessing ecological benefits and risks to species as well as effective management strategies. Further, fine-scale species-level and functional type mapping is important to monitor plant expansion, invasions, biodiversity, and ecosystem function. The objective of this study was to create an accurate species-level classification map using a combination of very high resolution (VRH) World View-3 multispectral and hand-held hyperspectral data acquired from a handheld radiometer and to assess the differences in accuracy assessment between pixel-based and object-based classification techniques. In order to identify how species classification in the landscape has changes and will continue to change, we need accurate, large-scale, baseline maps of species distribution to compare to future images. We compared pixel-based classification and object-based classification approaches using hyperspectral data and VHR multispectral data to determine what factors were most important for creating accurate species-level classifications. Overall, object-based classification had higher classification accuracy (0.915, kappa coefficient=0.905) than pixel-based classification (0.79, kappa coefficient=0.766). The most noticeable improvement with the object-based classifications was more effective differentiation between species within the same life form (shrubs, grasses, trees, etc.). Although the common vegetation indices, NDVI and GNDI, were effective for much of the species identification, other area metrics like number of pixels, density, shape, texture, length, and brightness, were necessary to distinguish between similar life forms. Results from this study demonstrate that while the pixel-based classification approach created fairly accurate species-level maps, classification was

improved upon by using training sites and an object oriented classification. The improvement in accuracy was due to other metrics besides reflectance used to differentiate species. If the mapping objective is to identify life forms, pixel based approaches would be sufficient. But to classify species within life forms, object based approaches were necessary.

Keywords: Colorado Plateau, World View-3, hyperspectral, multispectral, object-based classification, pixel-based classification

Introduction

Accurate species distribution mapping is crucial for assessing ecological changes in communities leading to effective management strategies (Ahrens *et al.* 2010). Ecosystem mapping has been important in monitoring biological invasions, global climate change, biodiversity, and fundamental ecosystem processes such as fire and nutrient cycling (National Research Council 1994; Mack 2005; Panetta & Lawes 2005; Herrick *et al.* 2010; Shouse *et al.* 2013; Calviño-Cancela *et al*. 2014; Gillian *et al.* 2014). Detection and mapping of species and communities is often based on field surveys. Although field surveys provide precise information about species relative cover, density, and composition (Stock *et al.* 2004; Adjorlolo *et al.* 2012), they are often time consuming and labor intensive (Jorgensen & Kollmann 2009; Ahrens *et al*. 2011; Calviño-Cancela *et al.* 2014) and can provide limited information, usually confined to small sampling areas (Panetta & Lawes 2005). Remote sensing techniques are popular for ecosystem assessments because of their lower total cost, greater coverage, and more regular data collection cycle while still being able to distinguish between similar categories, such as plant species (Calviño-Cancela *et al.* 2014). Using remote sensing technology to discriminate between

different plant species and functional types has been effective in better understanding local vegetation and ecosystem dynamics (Ehleringer & Monson 1993; Bredenkamp *et al.* 2002; Hamada *et al.* 2011; Adjorlolo *et al.* 2012; Ferreira *et al*. 2016).

Remote Sensing

While remote sensing technologies are useful in ecosystem assessments, they require researchers to determine the optimal spatial and spectral resolution for mapping vegetation properties which can often be challenging (Atkinson & Curran 1995; Curran & Atkinson 1999; Woodcock & Strahler 1987). The scale at which observations are made (i.e. the instantaneous field of view or pixel size) may or may not align well with the scale of biophysical processes, and target size (i.e. individual species, patches of a given species, etc.) will vary across ecosystems and with ecological questions and concerns (Feld *et al.* 2009; Fisher 1997, Turner *et al.*1989). Satellite open access data such as Landsat or MODIS, while beneficial for large-scale ecotype classification, is hampered by high spatial resolution (30 km) that is too broad for species-level classification. Recent advances in remote sensing systems, such as World View-3 (launched on August 13, 2014, 31cm panchromatic resolution, 1.24m multispectral resolution, 3.7m short wave infrared resolution) now provide very high resolution (VHR-multispectral resolution 2 x 2 m or lower (Nagendra and Rocchini (2008)) data for land cover mapping. The use of these finer scale, VHR data for remote detection of invasive species has been shown to be useful in detection of plant species which occupy contiguous patches and occur in clumps (Wan *et al*. 2014; Niphadkar *et al.* 2017). It is less certain whether these platforms are sufficient for the remote sensing of more heterogeneous landscapes and dispersed clustering (Hamada *et al.* 2010). However, VHR multispectral data paired with *in situ* hyperspectral data acquired from a hand-

held radiometer, can improve spectral signatures used to differentiate between plant species (Ferreira *et al.* 2016).

Remote sensing of vegetation is based on the physical properties of leaves and their interactions with electromagnetic energy. Leaf structures of most plants interact with solar energy in essential the same biophysical process: high absorption in visible (optimally red and blue) bands by leaf pigments (e.g. chlorophyll a, b and ß-carotene), high reflectance in near-infrared band from the spongy mesophyll, and relatively high absorption in middle infrared bands by leaf water content. Hence, there is little selection for differences in spectral reflectance patterns during speciation, making the classification of different species by reflectance challenging (Sims & Gamon 2002; Shouse *et al.* 2013; Calviño-Cancela *et al.* 2014). Distinguishing between plant species often demands a large number of spectral bands to detect subtle differences in reflectance patterns. Hyperspectral sensors (also known as imaging spectrometers) measure reflectance in many narrow, adjacent spectral bands (often >100 bands) so they can pick up subtle differences in reflectance patterns necessary to distinguish between plant species (Ustin *et al.* 2004; Underwood *et al.* 2006; Kokaly *et al.* 2009; Schaepman *et al.* 2009; He *et al.* 2011; Calviño-Cancela *et al.* 2014). Studies using multispectral satellite data, in conjunction with *in situ* hyperspectral data, have been able to derive valuable ecosystem information such as the characterization of dominant plant species, functional types, or successional stages (Ustin & Gamon 2010; Asner 2013; Laurin *et al.* 2016). Several researchers have found that for their applications, the most promising sensors for improving classified map accuracy, and even discriminating dominant plant species, are imaging spectrometers (DeFries 2008; Schmidtlein *et al.* 2012; Ustin & Gamon 2010; Ustin *et al.* 2004; Roth *et al.* 2015). In arid grassland ecosystems, remote sensing techniques have been effective in quantifying shrub

expansion, invasive species, grazing extents, and anthropogenic threats (Hamada *et al.* 2011; Berg *et al.* 2016; Stevens *et al.* 2016). These techniques are less commonly used to identify individual species than functional types or life forms (Hamada *et al.* 2011). This is likely due to the difficulty in classifying grass species that are senesced and their small size and spectral similarities (Marsett *et al.* 2006). The ability map individual species as well as functional types and life forms is necessary for precise determination of distribution as well as effective management strategies (Calviño-Cancela *et al.* 2014).

Image Classification

In an ecosystem with a mosaic of different species, ages, sizes, and degree of spatial heterogeneity, remote sensing image classification is largely determined by specific site information and variation (Zhang & Qiu 2011; Shouse *et al.* 2013; Laurin *et al.* 2016). In a typical image classification, individual pixels are assigned to real world classes based solely on their spectral characteristics (Newman *et al.* 2011). The most commonly used classification methods operate on individual pixels as the units of classification. These methods assign each pixel into classes according to classification algorithms or decision rules. Each individual pixel is analyzed according to its spectral characteristics, but this method does not consider the spatial characteristics of the surrounding pixels and their relationships to each other (Laliberte *et al.* 2004). A more recent approach to classification, developed around the year 2000 (Blaschke 2010), uses clusters of pixels, or 'image objects', as representations of objects on the ground. In object-based classification, image objects are categorized into classes based on multiple defined criteria. Segmentation of the entire image to create image objects is based on the size and type of the real-world objects to be identified. The remote sensing software, eCognition, allows the user

to define criteria in an image segmentation such as scale parameter, composition of homogeneity criterion for color and shape, and the shape criterion for smoothness and compactness to classify objects in an image. The size of each image is defined by the scale factor that is related to the image resolution. The color parameter controls the extent of spectral heterogeneity within the object. The shape parameter is derived from textural characteristics of compactness and smoothness of the pixels. Thus, segmentation mimics human interpretation and groups images into homogenous areas (Laliberte *et al.* 2004; Newman *et al.* 2011). Once segmented, images are classified according to the 'features' of each object. These features are the spectral shape and contextual characteristics of the image objects. In addition to reflectance values and mean brightness for each band, area, length, texture, width, shape, compactness and dozens of other features can be used to differentiate between pixel classes. Object-based classification permits the incorporation of contextual and spatial information, whereas pixel-based classification methods are based on spectral/layer pixel values. Due to the addition of these parameters in classification, an object based classification would be expected to provide superior results to spectral differentiation (Laliberte *et al.* 2004; Karl 2010; Laliberte *et al.* 2010; Duniway *et al.* 2011).

Combining several features of spectral, geometric, and textural information to classify images often outperform spectral vectors alone (Proctor *at al.* 2013; Fernandes *et al.* 2014). Some of the most fundamental indicators relevant to ecosystem services in grasslands and shrublands are ground cover (vegetation, rock, and litter cover) and vegetation community composition (Duniway *et al.* 2011). The development of the Normalized Difference Vegetation Index (NDVI), which measures live green plant materials using the red and near-infrared bands, quickly became the most dominant satellite observable metric for plant biomass and

photosynthetic activity. It has led to an increase in the number of studies looking at plant canopy reflectance (Houborg *et al.* 2015). However, in arid ecosystems, using a green index like NDVI, or other vegetation metrics like the greenness index, GNDVI, it is possible to misclassify grass species after their peak greenest (Marsett *et al.* 2006). Recent studies have suggested that object-based classification produces more accurate habitat maps than those classified using pixel-based methods (Clark *et al.* 2005; Hamada *et al.* 2011; Newman *et al.* 2011; Ferreira *et al.* 2016; Niphadkar *et al.* 2017). However, if the spectral signatures used to create the rule set for the pixel-based classification were created using hyperspectral data, the classification accuracy for the habitat map could potentially improve. Many of the studies that find improvement in object-based classification are mapping larger landscapes, ecotypes, functional classes, or growth forms. Species-level classification techniques are less common and the small-scale nature of the question might benefit from a more heavily weighted spectral classification.

Steep canyon walls, rocky terrain, and high species diversity make Canyonlands National Park on the Colorado Plateau an ideal place to conduct this research. Canyonlands is host to a diverse community of plant species with a clear, directional climate signal affecting key plant functional groups. Over time, researchers have seen shifts in community composition (Munson *et al* 2011a; 2011b; Hoover *et al.* 2017), due to differential responses to climate change. Plant functional types, specifically photosynthetic pathway, duration (annual or perennial), and life form (tree, shrub, forb, or grass) have been shown to confer benefits in climate changing conditions, (Munson *et al.* 2011a; Hoover *et al.* 2017; Duffy & Chown 2016). Canyonlands is host to conservation issues with invasive species, legacy effects from historic grazing, and declines in critical species, including desert grasses. Some locations within the national park are difficult to reach on foot and others are completely enclosed by canyon walls making field

sampling across a large area not feasible. Within United States national park boundaries, drones are not generally permitted making fine spatial imagery more difficult to acquire. However, there is a need for accurate species-level mapping of the ecosystem that can be generated over a large area. Important species can be tracked over time and changes in density and distribution can be monitored. Another feature of the location that adds complexity to our study is the heterogeneous size of the plant species. Species found in the site include trees with canopies much larger than WV-3 pixel sizes, shrub sizes around pixel sizes, and grasses that are much smaller than pixel size. Capturing the diversity of size, shape, and distribution of species in a map is a challenge with multispectral, satellite imagery.

Our goal in this project was to produce a high-resolution map of species distributions in a topographically and botanically diverse landscape. To achieve this goal, we pursued three specific aims: 1) Utilize reflectance curves created from species-specific hyperspectral data to improve pixel-level classification, 2) Compare pixel-level classification to object-level classification, and 3) Evaluate the importance of non-spectral related features used in object-based classification in improving overall accuracy. To achieve these aims, we assessed the feasibility and reliability of multiple remote sensing techniques to create a species-level classification map. We combined hyperspectral data from handheld spectral radiometers with multispectral data from the World View-3 satellite to build spectral signature curves and identify regions on the electromagnetic spectrum where each species could be separated from others. We used these values to create a rule set that we implemented in a spectral differentiation classification. We compared the accuracy assessment from the spectral differentiation to our object oriented classification using training sites. We also compared object attributes to determine whether reflectance values alone are sufficient for classifying species, and how other

features such as size, density, shape, and texture change the classification accuracy. While the question about classification accuracy has been addressed in other systems, the homogeneity of our study area combined with the size of the species we classified make this approach novel. Knowing what features and what techniques can be most successful to create accurate large-scale species-level classification maps will allow researchers to collect large-scale species distribution data in regions where in-situ sampling is not feasible.

Methods

Site Description

The study was conducted in the Needles District, the southeast corner of Canyonlands National Park, on the Colorado Plateau in Utah, U.S.A (Fig 1). Across the study area, there is high variation in topography from the tall spires of Cedar Mesa Sandstone forming canyon walls, coarse Aeolian deposits and flat to gently sloping alluvial silty soils. Vegetation in our site represent common desert plant species found in the arid southwest (Table 1).

Image Pre-processing

Images were acquired on June 29, 2015 and May 30, 2016 using the World View-3 satellite. The images were georeferenced by the USGS prior to our study. To begin the atmospheric correction using Fast Lane-of-sight Atmospheric Analysis of Spectral Hypercubes (FLAASH), we had to radiometrically calibrate the image from BSQ format to BIL output interleave with the calibration type set to “Radiance”, output data type set to “Float”, and the scale factor 0.1, according to FLAASH settings in ENVI. After the image was calibrated, we ran

the FLAASH atmospheric correlator. FLAASH accurately compensates for atmospheric effects by correcting wavelengths in the visible, near-infrared, and short-wave infrared regions.

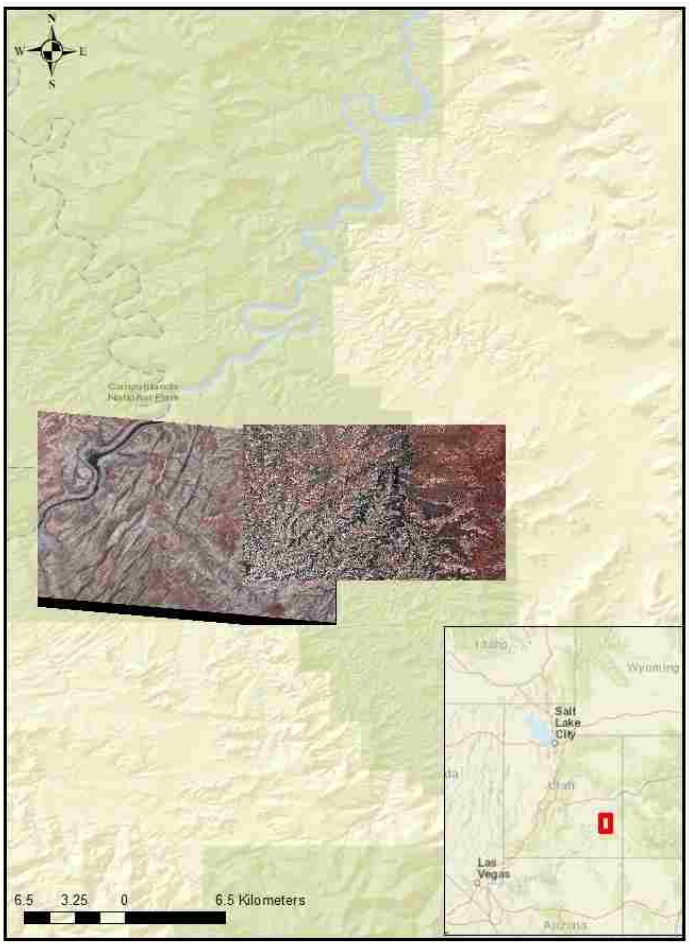

Figure 1 Study site
Map of study site in the Needles District of Canyonlands National Park on the Colorado Plateau. Images overlaid on the map are the World View-3 images. Across the study area, there is high variation in topography from the tall spires of Cedar Mesa Sandstone forming canyon walls, coarse Aeolian deposits and flat to gently sloping alluvial silty soils.

Table 1 Species measured

Common species found on the Colorado Plateau and sampled in the study. We used these species to measure spectral reflectance and also to take ground truth data with a GPS.

Common Name	Scientific Name	Lifeform	Pathway	Duration
Ambrosia	*Ambrosia dumosa*	Shrub	C3	Perennial
Big sagebrush	*Artemisia tridentata*	Shrub	C3	Perennial
Four Wing Saltbrush	*Atriplex canescens*	Shrub	C4	Perennial
Blue Grama	*Bouteloua gracilis*	Grass	C4	Perennial
Mountain Mahogany	*Cerocarpus betuloides*	Small tree	C3	Perennial
Rabbitbrush	*Chrysothamnus viscidiflorus*	Shrub	C3	Perennial
Blackbrush	*Coleogyne ramosissima*	Shrub	C3	Perennial
Mormon Tea	*Ephedra viridis*	Shrub	C3	Perennial
Torrey's Jointfir	*Ephedra torreyana*	Shrub	C3	Perennial
Needle and Thread	*Hesperostipa comata*	Grass	C3	Perennial
Juniper	*Juniperus osteoperma*	Tree	C3	Perennial
Common Pepperweed	*Lepidium densiflorum var. ramosum*	Forb	C3	Annual
Indian Rice Grass	*Oryzopsis hymenoides*	Grass	C3	Perennial
James' Galleta	*Pleuraphis jamesii*	Grass	C4	Perennial
Pinyon Pine	*Pinus monophylla*	Tree	C3	Perennial

Reflectance curves and pixel-based classification

We used the HandHeld2 Pro hand-held spectrometer (ASD Inc.) to measure 170 reflectance curves for seven common grass and shrub species from wavelength measurements of 325 nm to 1075 nm; each band had a bandwidth of less than 3.0 nm. The values were averaged for each species to account for variation across individuals. The hyperspectral sensor allowed for greater discrimination of species in areas along the electromagnetic spectrum where they grouped together (Figure 2). Then using sensor information from the WV-3 satellite, we identified the bandwidth where each color was picked up by the sensor (see vertical lines on Figure 2). These are the bands where each color on our image was picked up by the WV-3 satellite and which bands are useful in separating species from each other.

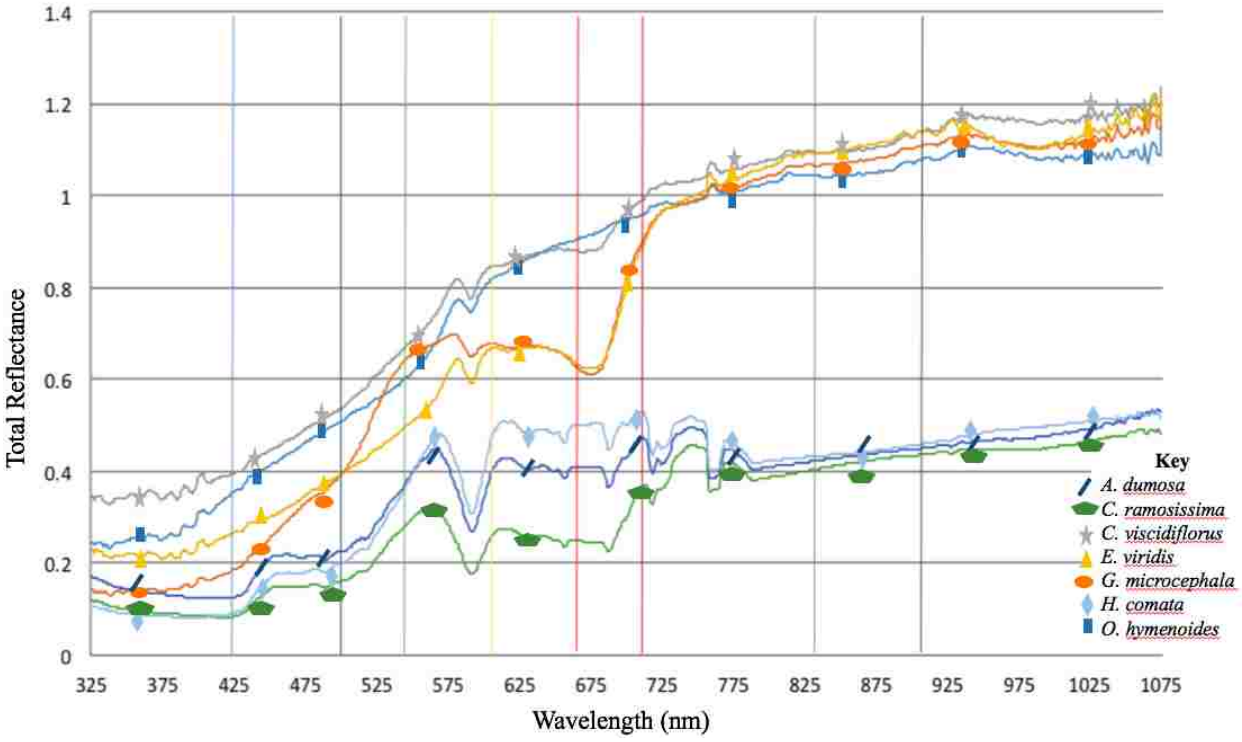

Figure 2 Spectral signatures
Measured wavelengths of light on the electromagnetic scale and the corresponding total reflectance for species. Vertical Bands represent where World View-3 sensors pick up reflectance for each color gun.

Ground Reference Data

Global Positioning System (GPS) points were measured for 281 large shrubs and patches of grass as well as bare ground and rocks using a Trimble GeoX GPS unit. We labeled the different elements of the terrain in areas where the invasive target species was abundant (with patches of different sizes and characteristics) and other representative elements (red rock, white rock, bare ground). Because of lack of accessibility to many areas blocked by canyon walls and far from roads or trails, not all areas within the images could be evenly sampled for ground reference data. We selected training pixels from these ground points to train the classifier. The dataset was randomly partitioned into 60% for training and 40% for testing. We repeated the

splitting ten times, randomly choosing reference points and testing the classifiers at each location to better assess the robustness of the classification and its ability to predict unknown samples.

Comparison of Approaches

Spectral Differentiation

Using the decision tree we created to separate species from each other based on specific wavelengths with the most separation distance, we created a spectral differentiation rule set in eCogntition Developer™ 9.0 Software. The rule set used only reflectance values and created a range that each species fit within according to the hyperspectral data taken from the hand-held reflectometer. We ran a classification on the images and determined the accuracy of the assessment using the ground points.

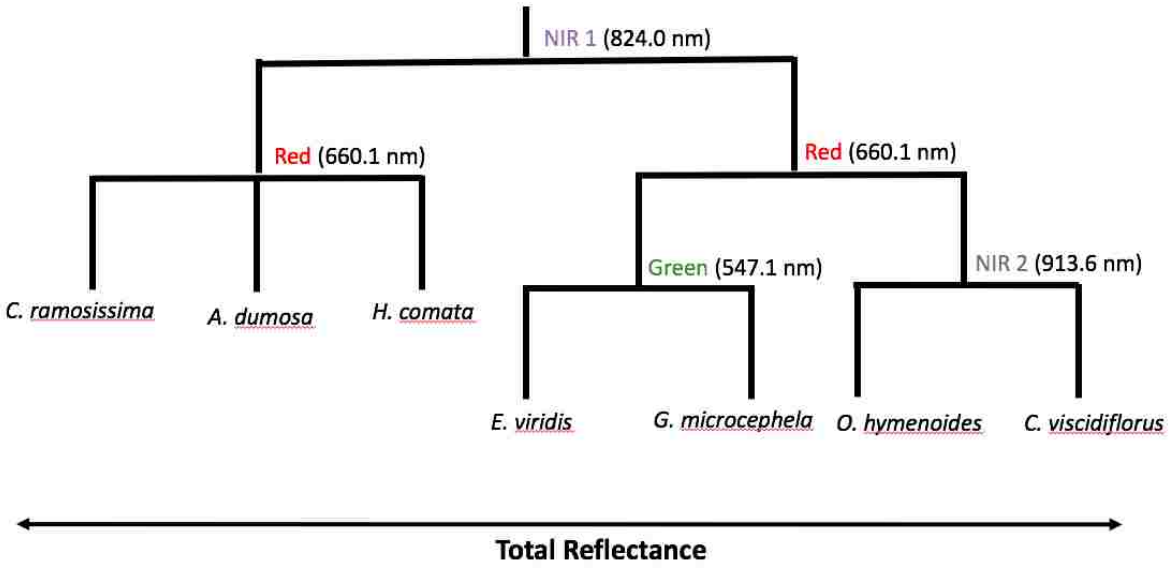

Figure 3 Spectral signature decision tree
Decision tree based on spectral signatures graphed in Figure 2. The decision tree works for creating a rule set in eCognition when running a spectral differentiation classification. As an example, if you wanted to map E. *viridis*, the WV-3 color guns you should use are NIR 1, then Red, and Green. *E. viridis* can be most easily separated from *G. microcephala* on the image at the wavelength 547.1 nm.

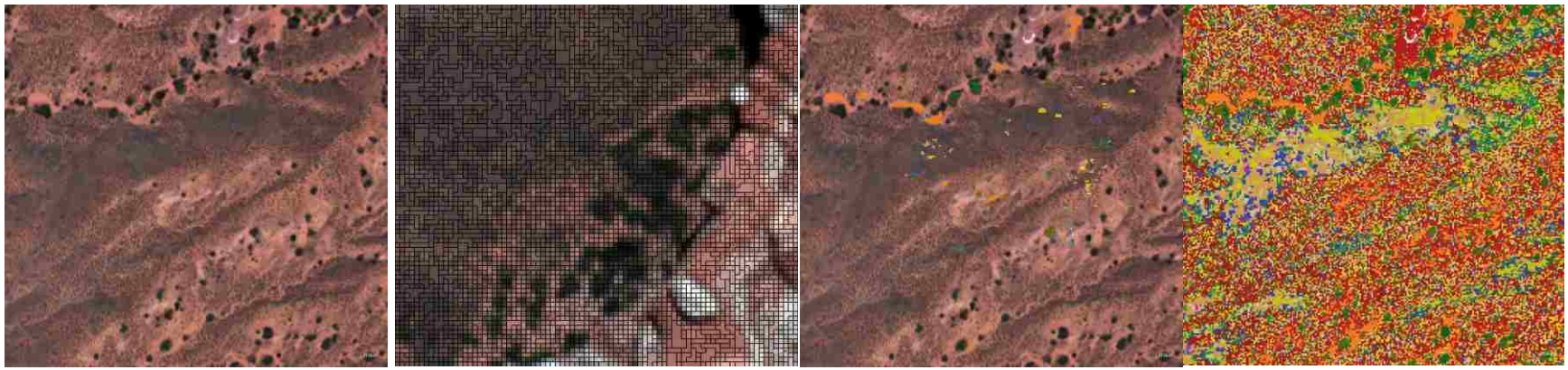

Figure 4 Image processing methods
Original World View-3 image (panel 1), segmented image (panel 2), image with object classes identified for one area of the region (panel 3), and classification (panel 4).

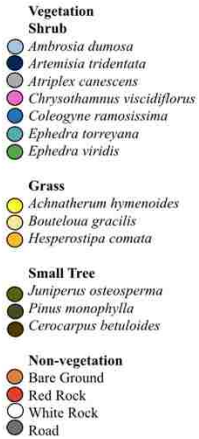

Object oriented classification

The second approach to creating a species-level classification was using the object-based classification approach in eCognition (Definiens 2010). Classification of remotely sensed imagery is the process of assigning pixels to discrete categories of terrain elements, i.e. one of the target plant species, red and white rock, and bare ground categories using training sites. Before running the classification, we ran a segmentation to subdivide the image into image objects or primitives (approximating ground targets, e.g. shrub patch) by clustering pixels into contiguous regions of minimum heterogeneity at a given scale (Benz *et al.* 2004). A multiresolution segmentation was used to optimize the mapping of ground features characterized by a wide range of sizes and shapes, from small clumps of shrubs to large patches of forest or pasture. Multiresolution segmentation is a bottom up region-growing technique starting with one-pixel objects and then in subsequent steps, merging smaller image objects into bigger ones. Throughout this pairwise clustering process, the underlying optimization procedure minimizes the weighted heterogeneity of resulting image objects. In each step, the pair of adjacent image objects is merged which stands for the smallest growth of the defined heterogeneity. If the smallest growth exceeds the threshold defined the scale parameter, the process stops. Doing so, multiresolution segmentation is a local optimization procedure. The segmentation used a low scale parameter (scale = 3) to delimit the smallest ground features. Segmentation at these scales tends to over-split medium-to-large ground features (e.g. large grass patches) into a large number of objects. Hence, we used a spectral difference segmentation to merge contiguous objects having similar mean reflectance values.

Important Features in Object-based classification

When classifying objects, eCognition uses object descriptors or 'features' to assign an object to a class using crisp or fuzzy transition functions, or by the application of nearest-neighbor membership functions trained by representative class samples (Benz *et al.* 2004). We applied both crisp rules and nearest-neighbor membership functions to assign objects to classes. For the latter, we selected between 10 and 30 object samples per class (depending on the abundance in the study area) as training references for the classification. The appropriate class for each training reference was determined from either field surveys or directly from the image. Four methods were considered for discriminating the land-cover classes in eCognition, namely (1) statistical (e.g. mean, standard deviation, ratios, and minimum and maximum of pixel values within an object); (2) textural (e.g. mean difference to neighbors); (3) contextual descriptors (e.g. mean difference of an object between inner and outer border or scene); (4) spectral indices for vegetation and bare ground characterization, such as NDVI and GNDVI (greenness index).

We assessed class separability and selected the best discriminating features using the feature space optimization tool in eCognition. This tool uses the training references to measure the statistical distance between classes for a set of features and displays a class separation distance matrix (Definiens 2010). A high separation distance between two classes suggests that the selected features can discriminate the two classes. A distance of J = 0 means complete correlation or low separability and J = 2 means complete non-correlation and high separability.

With the features selected for the classification, we next assigned training classes and points. We randomly selected training sites from within the ground truthing points to use in the classification. Fifteen non-vegetation and vegetation classes were mapped considering their likely discrimination in the scenes. Non-vegetation classes included white rock, red rock, road,

and bare ground. Vegetation classes included common species in the site: *Ambrosia dumosa*, *Atriplex canescens* (Four winged saltbrush), *Cerocarpus betuloides* (Mahogany), *Coleogyne ramosissima* (Blackbrush), *Ephedra torreyana* (Torrey's jointfir), *Ephedra viridis* (Mormon tea), *Chrysothamnus viscidiflorus* (Rabbitbrush), *Hesperostipa comata* (Needle and Thread grass), *Juniperus osteosperma* (Juniper), *Achnatherum hymenoides* (Indian Rice Grass), and *Pinus monophylla* (Pinyon Pine).

Accuracy Assessment

To assess the accuracy of image classification we compared the classified image with ground validation data and created an error matrix. We randomly selected 250 reference points taken from the field and compared their identification in the field with the image classification we created. We first measured overall accuracy. Overall accuracy is the proportion of all reference pixels, which ae classified correctly (in the sense that the class assignment of the classification and of the reference classification agree). It is computed by dividing the total number of correctly classified pixels (the sum of the elements along the main diagonal) by the total number of reference pixels. Overall accuracy is a very coarse measurement. It gives no information about what classes are classified with good accuracy.

We determined the rates of omission errors (or false negatives, when pixels with presence of a target species on the ground were not properly classified) and commission errors (or false positives, when pixels were classified as with presence of a target species that was absent on the ground) which define the producer's and user's accuracy, respectively. We also estimated the kappa coefficient, which provides a measure of the difference in agreement between the classified map and ground validated data against an agreement occurring by chance (Landis &

Koch 1977). Further, Kappa analysis is a discrete multivariate technique used in accuracy assessment for statistically determining if one error matrix is significantly different from another. The measure of agreement is based on the difference between the actual agreement in the error matrix (i.e. the agreement between the remote sensed classification and the reference data as indicated by the major diagonal) and the chance agreement, which is indicated by the row and column totals (i.e. marginals).

There is always a detection threshold related to the spatial resolution of the system and, for all species, there will always be individuals, e.g. seedlings or small plantings, that cannot be detected. Therefore, we were not able to sample small forb species and seedlings that covered less than 50% of our pixel size, i.e. 0.5 m^2 for images of $1m^2$ spatial resolution.

Results

Reflectance Curves and Pixel-based Classification

The reflectance curves created from hyperspectral data improved the pixel-based classification by providing more detailed rule sets for each species. Their accuracy is confirmed by the improvement in accuracy between the pixel-based (only reflectance data) and the object-based classification.

Compare pixel-level classification to object-level classification

Both spectral differentiation and object oriented classifications produced overall classification accuracies above 75%. The spectral differentiation had an overall accuracy of 79% (kappa coefficient=0.76) and the object oriented classification had an overall accuracy of 91% (kappa coefficient=0.90). For the producer's accuracy, there were improvements in the object

oriented classification compared to the spectral differentiation for eight species, no change for three species, and decline in two species. Species that improved in producer's accuracy with the object oriented classification were *P. monophylla* (from 0.6 to 0.85), *J. osteosperma* (from 0.58 to 0.84), *C. ramosissima* (from 0.57 to 0.95), *E. viridis* (from 0.8 to 0.94), *A. canescens* (0.76 to 0.88), *C. viscidiflorus* (0.87 to 0.88), *H. comata* (0.79 to 0.89), and *A. hymenoides* (0.84 to 0.93). Two species had slightly worse producer's accuracies with the object oriented classification than the spectral differentiation, *E. torreyana* (0.86 to 0.85), *A. dumosa* (0.76 to 0.72) (Figure 5 and Figure 6).

For the user's accuracy, there were improvements in the object oriented classification compared to the spectral differentiation for eight species, no change for three species, and decline in two species. Species that improved in user's accuracy with the object oriented classification were *P. monophylla* (from 0.75 to 0.85), *C. ramosissima* (from 0.84 to 0.96), *A. canescens* (0.82 to 0.95), and *C. viscidiflorus* (0.93 to 1), and a decline for *E. torreyana* (1 to 0.93), *A. dumosa* (0.9 to 0.8), *H. comata* (1 to 0.97), and *A. hymenoides* (0.88 to 0.87). Producer's and user's accuracies were in general very similar for species, with higher user's accuracy in both instances (0.88 for spectral differentiation and 0.92 for object oriented classification) compared to producer's accuracy (0.80 and 0.90).

Important Features in Object-based Classification

Overall, reflectance values for NDVI and GNDVI indices were fairly effective in classifying species (Figure 5), but the use of other features improved the classification (Figure 6). The differences can be seen in the class separation distance matrix (Table 2) and the sample editor table (Figure 3 for just NDVI values and Suppl. Fig S1 for complete table). In Table 3, we

can see that there are four instances where species completely overlap in the range of reflectance values when NDVI only was used in the classification. All four instances of complete overlap occurred between three grass species, and two lighter-colored shrubs (*H. comata, A. hymenoides, C. ramosissima, B. gracilis,* and *C. viscidiflorous*). Figure 4 shows alternative bands and metrics that can be used to differentiate plant species when there is overlap in a feature like NDVI. To differentiate between *B. gracilis* and *H. comata* (both grasses), *C. viscidiflorus* and *H. comata* (shrub and grass) and *C. ramosissima* and *A. hymenoides* (shrub and grass), mean brightness only overlaps by 0.19, 0.55, and 0 respectively. Brightness was not effective for *C. ramosissima* and *H. comata*, but mean NIR only had 0.28 overlap. Geometric metrics like size, width, length, and shape were effective in differentiating between different shrub species and also contrasting them with other lifeforms.

Figure 5 Classification map
Complete classification maps for both the front country and canyon regions of Canyonlands National Park.

Table 2 Pixel-based confusion matrix
Confusion matrix for the pixel-based, rule set and spectral differentiation analysis in eCognition.

Class/Class	P. monophylla	C. betuloides	J. osteosperma	Q. gambelii	C. ramosissima	E. viridis	E. torreyana	A. dumosa	A. canescens	C. viscidiflorus	H. comata	O. hymenoides	Bare Ground	Unclassified	Row Total	Accuracy
P. monophylla	3	0	0	0	0	0	0	0	0	0	0	0	0	2	5	0.6
C. betuloides	0	2	0	0	0	0	0	0	0	0	0	0	0	0	2	1
J. osteosperma	1	0	7	0	0	0	0	0	2	0	0	0	0	2	12	0.58333333
Q. gambelii	0	0	0	5	0	0	0	0	0	0	0	0	0	0	5	1
C. ramosissima	0	0	0	0	11	1	0	1	2	0	0	0	0	4	19	0.57894737
E. viridis	0	0	0	0	1	38	0	0	0	0	0	0	0	8	47	0.80851064
E. torreyana	0	0	0	0	0	1	13	0	0	0	0	0	0	1	15	0.86666667
A. dumosa	0	0	0	0	0	0	0	10	0	0	0	0	0	3	13	0.76923077
A. canescens	0	0	0	0	1	1	0	0	19	0	0	0	0	4	25	0.76
C. viscidiflorus	0	0	0	0	0	0	0	0	0	14	0	0	0	2	16	0.875
H. comata	0	0	0	0	0	0	0	0	0	0	27	2	0	5	34	0.79411765
O. hymenoides	0	0	0	0	0	0	0	0	0	1	0	32	0	5	38	0.84210526
Bare Ground	0	0	0	0	0	0	0	0	0	0	0	0	3	0	3	1
Unclassified	0	0	0	0	0	0	0	0	0	0	0	2	0	12	14	0.85714286
Column Total	4	2	7	5	13	41	13	11	23	15	27	36	3	48		
Reliability	0.75	1	1	1	0.846153846	0.9268293	1	0.909090909	0.826086957	0.933333333	1	0.888888889	1	0.25		

Overall Accuracy	0.79032
Kappa Coefficient	0.76867
Producer's Accuracy	0.80965
User's Accuracy	0.88074

Table 3 Object-based confusion matrix
Confusion matrix for the object-based classification using training sites in eCognition.

Class/Class	P. monophylla	C. betuloides	J. osteosperma	Q. gambelii	C. ramosissima	E. viridis	E. torreyana	A. dumosa	A. canescens	C. viscidiflorus	H. comata	O. hymenoides	Bare Ground	Unclassified	Row Total	Accuracy
P. monophylla	6	0	0	0	0	0	0	0	0	0	0	0	0	1	7	0.85714286
C. betuloides	0	2	0	0	0	0	0	0	0	0	0	0	0	0	2	1
J. osteosperma	1	0	11	0	0	0	0	0	1	0	0	0	0	0	13	0.84615385
Q. gambelii	0	0	0	5	0	0	0	0	0	0	0	0	0	0	5	1
C. ramosissima	0	0	0	0	23	1	0	0	0	0	0	0	0	0	24	0.95833333
E. viridis	0	0	0	0	0	37	0	0	0	0	0	0	0	2	39	0.94871795
E. torreyana	0	0	0	0	0	1	15	0	0	0	0	0	0	0	14	0.78571429
A. dumosa	0	0	0	0	0	1	1	8	0	0	0	0	0	1	11	0.72727273
A. canescens	0	0	0	0	1	0	0	2	22	0	0	0	0	0	25	0.88
C. viscidiflorus	0	0	0	0	0	0	0	0	0	8	0	0	0	1	9	0.88888889
H. comata	0	0	0	0	0	0	0	0	0	0	34	2	0	2	38	0.89473684
O. hymenoides	0	0	0	0	0	0	0	0	0	0	1	27	0	1	29	0.93103448
Bare Ground	0	0	0	0	0	0	0	0	0	0	0	0	5	0	5	1
Unclassified	0	0	0	0	0	0	0	0	0	0	0	2	0	15	17	0.88235294
Column Total	7	2	11	5	24	40	16	10	23	8	35	31	5	23	238	
Reliability	0.857142857	1	1	1	0.958333333	0.925	0.9375	0.8	0.956521739	1	0.971428571	0.870967742	1	0.652173913		

Overall Accuracy	0.91596
Kappa Coefficient	0.90676
Producer's Accuracy	0.90002487
User's Accuracy	0.92350487

The values within the class separation distance matrix inform us how much separation there is between species pixel values for all of the combined factors in the classification. 0 indicates no separation and higher numbers indicate higher separation. The values below 2, the benchmark set for sufficient separability are *C. viscidiflourus* and *E. torreyana* (1.87), *C. viscidiflourus* and *A. hymenoides* (1.15), *J. osteosperma* and *P. monophylla* (1.26), and *E. viridis* and *E. torreyana* (1.29) (see Table 2).

In the Average Nearest Neighbor analysis, we see that the distribution of species in the landscape is not due to chance. The expected mean difference between species was 0.577m and the observed mean distance was 1.03 m. With a z-score of 2320.47 and a p-value of <0.001, there is less than a 1% chance that the dispersal pattern witnessed in the site is due to chance.

Table 4 Class separation distance matrix

Class Separation Distance Matrix for object-based classification. The values represent the amount of separation between two species in the image using all of the image object related features in the object-based classification. A value of 2 is generally accepted as the benchmark for separating between species. More than 2 units of separation between species is deemed sufficient for accurately separating them. From 0-2 is not the most ideal separation. Species can still be differentiated but it is more difficult.

Class/Class	***A. tridentata***	***A. canescens***	**Bare Ground**	***B. gracilis***	***C. viscidiflorus***	***C. ramosissima***	***E. torreyana***	***E. viridis***	***H. comata***	***J. osteosperma***	***A. hymenoides***	***P. monophyla***	**Red Rock**	**Road**	**White Rock**
A. tridentata	0														
A. canescens	3.597957	0													
Bare Ground	18.798298	9.504423	0												
B. gracilis	11.148174	5.656309	15.635604	0											
C. viscidiflorus	5.602458	2.42932	16.648042	2.787529	0										
C. ramosissima	17.688781	15.787685	20.437673	17.248157	17.125904	0									
E. torreyana	6.012781	3.16641	13.529162	2.222371	1.874773	12.372592	0								
E. viridis	3.903661	3.120262	16.336391	3.943448	2.300185	14.233153	1.193336	0							
H. comata	5.948544	2.155921	6.978308	6.393288	3.970894	12.942281	3.820866	5.261408	0						
J. osteosperma	4.080788	6.838284	18.231344	16.249151	9.833356	24.956844	11.653387	7.08443	8.242005	0					
A. hymenoides	5.136762	2.138177	9.108365	2.215567	1.15342	17.935609	2.021818	2.791877	2.014733	9.458255	0				
P. monophyla	4.144869	7.793742	17.813204	16.488712	10.542592	26.192191	12.364177	9.04341	9.299724	1.261062	10.295789	0			
Red Rock	15.084899	9.060893	3.154298	9.121408	10.76909	21.406476	7.897792	9.611497	6.714601	15.499927	6.01782	13.723144	0		
Road	12.381036	8.842366	20.060391	18.252177	13.176859	26.005876	14.935734	14.546	12.772127	17.617183	13.089019	17.328866	11.809875	0	
White Rock	29.566601	24.091286	16.360871	22.961975	23.824595	37.951618	21.84081	24.35151	21.288614	31.651687	19.187892	25.509138	3.373638	9.046635	0

Table 5 Object overlap values

Object Oriented Classification object overlap values taken from the Sample Editor for NDVI values from a 0 to 1 scale with 0 being no overlap between NDVI ranges and 1 being complete overlap. There is strong overlap with NDVI levels between the grass species *H. comata* and the grass species *B. gracilis*, the shrub species, *C. ramosissima*, and *C. viscidiflorus*. This likely means there is a large NDVI range for *H. comata* and an inability by the NDVI matrix alone to differentiate between these species.

Class	***A. tridentata***	***A. canescens***	***B. gracilis***	***C. viscidiflorus***	***C. ramosissima***	***E. viridis***	***H. comata***	***J. osteosperma***	***O. hymenoides***	***P. monophylla***
A. tridentata	0	0.52	0.1	0.27	0.04	0.63	0.34	0.39	0.29	0.36
A. canescens		0	0.03	0.15	0.01	0.28	0.37	0.39	0.23	0.18
B. gracilis			0	0.55	0	0.47	1	0	0.82	0.2
C. viscidiflorus				0	0.07	0.53	1	0.21	0.5	0.05
C. ramosissima					0	0.02	1	0	1	0
E. viridis						0	0.24	0.45	0.13	0.3
H. comata							0	0.1	0.46	0.07
J. osteosperma								0	0.02	0.34
O. hymenoides									0	0.1
P. monophylla										0

Table 6 Other features that can be used to increase separation distance

This table displays other factors that can be used to differentiate between species with similar greenness (NDVI and GNDVI). The species shown here are the species with 100% overlap in NDVI range. There are other factors where they are quite different from each other, shown by lower overlap values. Weighing that color band more heavily or a feature like brightness, can emphasize these differences and allow for better discrimination. This is an advantage of object-based classification over pixel-based classification.

Species	**Brightness**	**Mean Red**	**Mean NIR 1**	**Mean Green**	**Mean Blue**	**Mean NIR 2**	**Mean Coastal**	**Mean Yellow**	**Max Difference**	**NDVI**	**GNDVI**
B. gracilis-H. comata	0.19	0	1	1	1	1	1	1	0.88	1	1
C. viscidiflorus-H. comata	0.55	0.42	0.75	1	1	0.88	0.85	0.5	0.88	1	1
C. ramosissima-H. comata	1	1	0.28	1	1	0.88	0.85	0.89	0.73	1	0.97
C. ramosissima-O. hymenoides	0	0.09	0	0.63	1	0	1	0.86	0.28	1	0.07

Discussion

We were able to successfully use VHR imagery to create the first accurate, park-wide map that shows the species-level distribution of dominant plants on the Colorado Plateau (Figure 5). These maps will serve as a baseline for future comparisons of species-level distributions over time and changes brought about by shifts in global climate. From the maps we can see that there is structure to where species exist. Chesler Park is pictured because it is geologically interesting and representative of regions on the Colorado Plateau. It is also a critical area for tourism with popular hikes and jeep trails. From the classification map, we can see that the rock fins surrounding the park are host to the larger tree species, *P. monophylla* and *J. ostesosperma* with an occasional deep-rooted shrub such as *E. viridis*, *E. torreyana*, and *C. ramosissima*. Sand ramps along the edge of the rock fins have fewer tree species and are replaced predominantly by shrub species. In the deep, silty soils of the inner canyon, grasses are the domain functional group.

Classification Accuracy

Overall, both classification methods were successful for large bunchgrasses and shrubs which is helpful for tracking the increase in shrub densities and the decrease in grasses. With the inclusion of roads, rock, and vegetation in the segmentation and classification, the object-based classification produced more accurate land-cover maps that better represented the plant class than the pixel-based classification methods did. For an object-based classification, the results of an accuracy assessment reflect not only the accuracy in the classification technique (e.g. the selection of features used to differentiate between the classes), but also the results of the initial segmentation of the image (Liu *et al.* 2008; Newman *et al.* 2011). Due to the spatial resolution of the imagery and the heterogeneity of the species distribution, the best segmentation used pixel

sizes of three. Slightly larger and the classification was largely successful but missed much of the detail found in the landscape and thus compromised the accuracy of the classification.

We obtained a good discrimination between classes (even for those with very similar reflectance patterns) in uniform areas where one particular class occupied entire pixels. The greatest overall improvements from the pixel-based classification to the object-based classification were found in classifying *P. monophylla* vs. *J. osteosperma*. Both highly photosynthetic species were difficult to differentiate in the pixel-based classification but were much better in the object-based classification. *C. ramosissima* also benefited from the object-based classification. In the pixel-based classification, several *C. ramosissima* were classified as *A. dumosa* and *A. canescens*, species with similar NDVI and peak reflectance values. In these cases, size metrics are important in differentiating between the species. Size, area, thickness, volume, and length all had almost negligible overlap values (0.05) which likely explains the improvement in accuracy assessment for the object-based classification. Another way to consider the correct classification of species is to notice the reduction of species incorrectly classified as 'unclassified'. In the pixel-based classification, there was a low user's accuracy for the unclassified pixels. This means that we incorrectly classified species as unclassified frequently.

For the grass species, there was improvement in correctly classifying species. In the pixel-based classification, there was an overestimation of *A. hymenoides*. Grass species were generally classified as grasses but not necessarily the correct species. The improvement in the object based classification occurred because of differences in brightness and max difference in pixel values, which had little overlap.

Limitations of the method

While the WV-3 satellite imagery was able to discriminate between major species of grasses, trees, and shrubs, the spatial resolution was still not fine enough to classify forbs and seedlings in the landscape. For a complete, inclusive species-level map, more fine resolution imagery would be required. Detection errors occurred when small individuals were located within or nearby large patches of another species. In these cases, the individual was often classified with the larger group. In practice, this shortcoming could influence the ability of remote sensing classifications to correctly identify species that benefit from close spatial distribution with shrubs. This 'island effect' finds hotspots of biological activity around shrubs that are able to pull moisture from deep within the soil profile that can then be used by species with shorter root systems. While our classification often identified these occurrences, more fine spatial resolution would aid in classifying species in these instances.

Considering the small size of a newly-emerged seedling, there are always individuals that will pass undetected regardless of the spatial resolution of the detection technique used. Because our site is classified as a perennial grassland with shrubs, most of the species are well-established bunch grasses or large shrubs, so missing seedlings is not too worrisome for a general classification mapping. Periodic image acquisition combined with *in situ* sampling in accessible regions would do well to improve upon the classification and track changes over time for species in the landscape. In addition, seedlings missed by earlier classifications can be detected in subsequent campaigns, once they exceed the size threshold for detection.

Implications

Arid ecosystems present different challenges in remote sensing of the landscape. There is less variation in heights of species and rarely are species stacked on top of each other as you would see in forest ecosystems. However, the size of the individual, their proximity to each other, and the interspaces prove to be challenges in classifying species in arid ecosystems. Duniway *et al.* (2011) said that remote sensing techniques have shown promise for measuring plant community composition and ground cover efficiently, but to applied to more large-scale surveys, it is necessary that they are feasible, cost-effective, and repeatable. That is the criteria we attempted to maintain in this project. While there are platforms with more fine spatial and spectral resolution, such as very-high-resolution imagery (~1mm ground sampling distance (GSD)), the equipment necessary for the analysis is not commonly available or affordable (Duniway *et al.* 2011). This research sheds light on the trade-off between imagery sufficient enough to discern major plant species but broad enough to fit the time and cost criteria stated above. We can see limitations of the data collected but also informative results that can lead to better landscape management and understanding of ecological phenomena. Berg *et al.* (2016) found that woody shrub encroachment underwent a major redistribution across the landscape. Shrub expansion did not occur equally or randomly across the landscape but was concentrated in formerly open, grassy areas. In previously wooded areas, there was no change or a reduction in shrub cover. With more findings like this, and a consistent mapping of open areas and woody areas, we can predict where shrub expansion will occur and other important ecological questions.

References

Adjorlolo, C., Mutanga, O., Cho, M.A., & Ismail, R. (2012). Challenges and opportunities in the use of remote sensing for C-3 and C-4 grass species discrimination and mapping. *African Journal of Range & Forage Science, 29*, 47-61

Ahrens, C., Chung, J., Meyer, T., & Auer, C. (2011). Bentgrass Distribution Surveys and Habitat Suitability Maps Support Ecological Risk Assessment in Cultural Landscapes. *Weed Science, 59*, 145-154

Alonzo, M., Bookhagen, B., & Roberts, D.A. (2014). Urban tree species mapping using hyperspectral and lidar data fusion. *Remote Sensing of Environment, 148*, 70-83

Asner, G.P. (2013). n Biological Diversity Mapping Comes of Age. *Remote Sensing, 5*, 374-376

Berg, M.D., Wilcox, B.P., Angerer, J.P., Rhodes, E.C., & Fox, W.E. (2016). Deciphering rangeland transformation-complex dynamics obscure interpretations of woody plant encroachment. *Landscape Ecology, 31*, 2433-2444

Booth, D.T., & Cox, S.E. (2008). Image-based monitoring to measure ecological change in rangeland. *Frontiers in Ecology and the Environment, 6*, 185-190

Bredenkamp, G.J., Spada, F., & Kazmierczak, E. (2002). On the origin of northern and southern hemisphere grasslands. *Plant Ecology, 163*, 209-229

Calvino-Cancela, M., Mendez-Rial, R., Reguera-Salgado, J., & Martin-Herrero, J. (2014). Alien Plant Monitoring with Ultralight Airborne Imaging Spectroscopy. *Plos One, 9*, 9

Carlson, K.M., Asner, G.P., Hughes, R.F., Ostertag, R., & Martin, R.E. (2007). Hyperspectral remote sensing of canopy biodiversity in Hawaiian lowland rainforests. *Ecosystems, 10*, 536-549

Clark, M.L., Roberts, D.A., & Clark, D.B. (2005). Hyperspectral discrimination of tropical rain forest tree species at leaf to crown scales. *Remote Sensing of Environment, 96*, 375-398

Dalponte, M., Orka, H.O., Gobakken, T., Gianelle, D., & Naeesset, E. (2013). Tree Species Classification in Boreal Forests With Hyperspectral Data. *Ieee Transactions on Geoscience and Remote Sensing, 51*, 2632-2645

DeFries, R. (2008). Terrestrial Vegetation in the Coupled Human-Earth System: Contributions of Remote Sensing. *Annual Review of Environment and Resources, 33*, 369-390

Dennison, P.E., & Roberts, D.A. (2003). The effects of vegetation phenology on endmember selection and species mapping in southern California chaparral. *Remote Sensing of Environment, 87*, 295-309

Duniway, M.C., Karl, J.W., Schrader, S., Baquera, N., & Herrick, J.E. (2012). Rangeland and pasture monitoring: an approach to interpretation of high-resolution imagery focused on observer calibration for repeatability. *Environmental Monitoring and Assessment, 184*, 3789-3804

Ehleringer, J.R., & Monson, R.K. (1993). EVOLUTIONARY AND ECOLOGICAL ASPECTS OF PHOTOSYNTHETIC PATHWAY VARIATION. *Annual Review of Ecology and Systematics, 24*, 411-439

Fernandes, M.R., Aguiar, F.C., Silva, J.M.N., Ferreira, M.T., & Pereira, J.M.C. (2014). Optimal attributes for the object based detection of giant reed in riparian habitats: A comparative study between Airborne High Spatial Resolution and WorldView-2 imagery. *International Journal of Applied Earth Observation and Geoinformation, 32*, 79-91

Ferreira, M.P., Zortea, M., Zanotta, D.C., Shimabukuro, Y.E., & de Souza, C.R. (2016). Mapping tree species in tropical seasonal semi-deciduous forests with hyperspectral and multispectral data. *Remote Sensing of Environment, 179*, 66-78

Gil, A., Yu, Q., Abadi, M., & Calado, H. (2014). USING ASTER MULTISPECTRAL IMAGERY FOR MAPPING WOODY INVASIVE SPECIES IN PICO DA VARA NATURAL RESERVE (AZORES ISLANDS, PORTUGAL). *Revista Arvore, 38*, 391-401

Gillan, J.K., Karl, J.W., Duniway, M., & Elaksher, A. (2014). Modeling vegetation heights from high resolution stereo aerial photography: An application for broad-scale rangeland monitoring. *Journal of Environmental Management, 144*, 226-235

Goodenough, D.G., Dyk, A., Niemann, O., Pearlman, J.S., Chen, H., Han, T., Murdoch, M., & West, C. (2003). Processing Hyperion and ALI for forest classification. *Ieee Transactions on Geoscience and Remote Sensing, 41*, 1321-1331

Hamada, Y., Stow, D.A., & Roberts, D.A. (2011). Estimating life-form cover fractions in California sage scrub communities using multispectral remote sensing. *Remote Sensing of Environment, 115*, 3056-3068

He, K.S., Rocchini, D., Neteler, M., & Nagendra, H. (2011). Benefits of hyperspectral remote sensing for tracking plant invasions. *Diversity and Distributions, 17*, 381-392

Herrick, J.E., Brown, J.R., Bestelmeyer, B.T., Andrews, S.S., Baldi, G., Davies, J., Duniway, M., Havstad, K.M., Karl, J.W., Karlen, D.L., Peters, D.P.C., Quinton, J.N., Riginos, C., Shaver, P.L., Steinaker, D., & Twomlow, S. (2012a). Revolutionary Land Use Change in the 21st Century: Is (Rangeland) Science Relevant? *Rangeland Ecology & Management, 65*, 590-598

Herrick, J.E., Duniway, M.C., Pyke, D.A., Bestelmeyer, B.T., Wills, S.A., Brown, J.R., Karl, J.W., & Havstad, K.M. (2012b). A holistic strategy for adaptive land management. *Journal of Soil and Water Conservation, 67*, 105A-113A

Herrick, J.E., Lessard, V.C., Spaeth, K.E., Shaver, P.L., Dayton, R.S., Pyke, D.A., Jolley, L., & Goebel, J.J. (2010). National ecosystem assessments supported by scientific and local knowledge. *Frontiers in Ecology and the Environment, 8*, 403-408

Holmes, K.W., Griffin, E.A., & Odgers, N.P. (2015). Large-area spatial disaggregation of a mosaic of conventional soil maps: evaluation over Western Australia. *Soil Research, 53*, 865-880

Houborg, R., Fisher, J.B., & Skidmore, A.K. (2015). Advances in remote sensing of vegetation function and traits. *International Journal of Applied Earth Observation and Geoinformation, 43*, 1-6

Humplik, J.F., Lazar, D., Husickova, A., & Spichal, L. (2015). Automated phenotyping of plant shoots using imaging methods for analysis of plant stress responses - a review. *Plant Methods, 11*, 10

Hunt, E.R., Everitt, J.H., Ritchie, J.C., Moran, M.S., Booth, D.T., Anderson, G.L., Clark, P.E., & Seyfried, M.S. (2003). Applications and research using remote sensing for rangeland management. *Photogrammetric Engineering and Remote Sensing, 69*, 675-693

Jakubauskas, M., Kindscher, K., & Debinski, D. (2001). Spectral and biophysical relationships of montane sagebrush communities in multi-temporal SPOT XS data. *International Journal of Remote Sensing, 22*, 1767-1778

Jorgensen, R.H., & Kollmann, J. (2009). Invasion of coastal dunes by the alien shrub Rosa rugosa is associated with roads, tracks and houses. *Flora, 204*, 289-297

Karl, J.W., Duniway, M.C., Nusser, S.M., Opsomer, J.D., & Unnasch, R.S. (2012a). Using Very-Large-Scale Aerial Imagery for Rangeland Monitoring and Assessment: Some Statistical Considerations. *Rangeland Ecology & Management, 65*, 330-339

Karl, J.W., Duniway, M.C., & Schrader, T.S. (2012b). A Technique for Estimating Rangeland Canopy-Gap Size Distributions From High-Resolution Digital Imagery. *Rangeland Ecology & Management, 65*, 196-207

Karl, J.W., Duniway, M.C., & Schrader, T.S. (2012c). A Technique for Estimating Rangeland Canopy-Gap Size Distributions From High-Resolution Digital Imagery. *Rangeland Ecology & Management, 65*, 196-207

Karl, J.W., Gillan, J.K., Barger, N.N., Herrick, J.E., & Duniway, M.C. (2014). Interpretation of high-resolution imagery for detecting vegetation cover composition change after fuels reduction treatments in woodlands. *Ecological Indicators, 45*, 570-578

Karl, J.W., Herrick, J.E., & Browning, D.M. (2012d). A Strategy for Rangeland Management Based on Best Available Knowledge and Information. *Rangeland Ecology & Management, 65*, 638-646

Kokaly, R.F., Asner, G.P., Ollinger, S.V., Martin, M.E., & Wessman, C.A. (2009). Characterizing canopy biochemistry from imaging spectroscopy and its application to ecosystem studies. *Remote Sensing of Environment, 113*, S78-S91

Kokaly, R.F., Despain, D.G., Clark, R.N., & Livo, K.E. (2003). Mapping vegetation in Yellowstone National Park using spectral feature analysis of AVIRIS data. *Remote Sensing of Environment, 84*, 437-456

Laliberte, A.S., Browning, D.M., Herrick, J.E., & Gronemeyer, P. (2010). Hierarchical object-based classification of ultra-high-resolution digital mapping camera (DMC) imagery for rangeland mapping and assessment. *Journal of Spatial Science, 55*, 101-115

Laliberte, A.S., Rango, A., Havstad, K.M., Paris, J.F., Beck, R.F., McNeely, R., & Gonzalez, A.L. (2004). Object-oriented image analysis for mapping shrub encroachment from 1937 to 2003 in southern New Mexico. *Remote Sensing of Environment, 93*, 198-210

Landis, J.R., & Koch, G.G. (1977). MEASUREMENT OF OBSERVER AGREEMENT FOR CATEGORICAL DATA. *Biometrics, 33*, 159-174

Laurin, G.V., Puletti, N., Hawthorne, W., Liesenberg, V., Corona, P., Papale, D., Chen, Q., & Valentini, R. (2016). Discrimination of tropical forest types, dominant species, and mapping of functional guilds by hyperspectral and simulated multispectral Sentinel-2 data. *Remote Sensing of Environment, 176*, 163-176

Li, Z.Q., Xu, D.D., & Guo, X.L. (2014). Remote Sensing of Ecosystem Health: Opportunities, Challenges, and Future Perspectives. *Sensors, 14*, 21117-21139

Liu, Y., Guo, Q.H., & Kelly, M. (2008). A framework of region-based spatial relations for non-overlapping features and its application in object based image analysis. *Isprs Journal of Photogrammetry and Remote Sensing, 63*, 461-475

Mack RN (2005) Assessing biotic invasions in time and space: The second imperative. In: Mooney HA, Mack RN, McNeely JA, Neville LE, Schei PJ, Waage JK, editors. Invasive Alien Species: A New Synthesis. Washington: Island Press. 179–208.

Magiera, A., Feilhauer, H., Tephnadze, N., Waldhardt, R., & Otte, A. (2016). Separating reflectance signatures of shrub species - a case study in the Central Greater Caucasus. *Applied Vegetation Science, 19*, 304-315

Marsett, R.C., Qi, J.G., Heilman, P., Biedenbender, S.H., Watson, M.C., Amer, S., Weltz, M.,

Goodrich, D., & Marsett, R. (2006). Remote sensing for grassland management in the arid Southwest. *Rangeland Ecology & Management, 59*, 530-540

Marshall, V.M., Lewis, M.M., & Ostendorf, B. (2014). Detecting new Buffel grass infestations in Australian arid lands: evaluation of methods using high-resolution multispectral imagery and aerial photography. *Environmental Monitoring and Assessment, 186*, 1689-1703

Martin, M.E., Newman, S.D., Aber, J.D., & Congalton, R.G. (1998). Determining forest species composition using high spectral resolution remote sensing data. *Remote Sensing of Environment, 65*, 249-254

Mueller-Warrant, G.W., Whittaker, G.W., & Young, W.C. (2008). GIS analysis of spatial clustering and temporal change in weeds of grass seed crops. *Weed Science, 56*, 647-669

Mullerova, J., Pergl, J., & Pysek, P. (2013). Remote sensing as a tool for monitoring plant invasions: Testing the effects of data resolution and image classification approach on the detection of a model plant species Heracleum mantegazzianum (giant hogweed). *International Journal of Applied Earth Observation and Geoinformation, 25*, 55-65

Nagendra, H., & Rocchini, D. (2008). High resolution satellite imagery for tropical biodiversity studies: the devil is in the detail. *Biodiversity and Conservation, 17*, 3431-3442

National Research Council, 1994 National Research Council Rangeland Health: New Methods to Classify, Inventory, and Monitor Rangelands National Academy Press, Washington, D.C (1994)

Newman, M.E., McLaren, K.P., & Wilson, B.S. (2011). Comparing the effects of classification techniques on landscape-level assessments: pixel-based versus object-based classification. *International Journal of Remote Sensing, 32*, 4055-4073

Niphadkar, M., Nagendra, H., Tarantino, C., Adamo, M., & Blonda, P. (2017). Comparing Pixel and Object-Based Approaches to Map an Understorey Invasive Shrub in Tropical Mixed Forests. *Frontiers in Plant Science, 8*, 18

Nouri, H., Beecham, S., Anderson, S., & Nagler, P. (2014). High Spatial Resolution WorldView-2 Imagery for Mapping NDVI and Its Relationship to Temporal Urban Landscape Evapotranspiration Factors. *Remote Sensing, 6*, 580-602

Ozdemir, I., & Karnieli, A. (2011). Predicting forest structural parameters using the image texture derived from WorldView-2 multispectral imagery in a dryland forest, Israel. *International Journal of Applied Earth Observation and Geoinformation, 13*, 701-710

Panetta, F.D., & Lawes, R. (2005). Evaluation of weed eradication programs: the delimitation

of extent. *Diversity and Distributions, 11*, 435-442

Papes, M., Tupayachi, R., Martinez, P., Peterson, A.T., & Powell, G.V.N. (2010). Using hyperspectral satellite imagery for regional inventories: a test with tropical emergent trees in the Amazon Basin. *Journal of Vegetation Science, 21*, 342-354

Petrou, Z.I., Manakos, I., Stathaki, T., Mucher, C.A., & Adamo, M. (2015a). Discrimination of Vegetation Height Categories With Passive Satellite Sensor Imagery Using Texture Analysis. *Ieee Journal of Selected Topics in Applied Earth Observations and Remote Sensing, 8*, 1442-1455

Petrou, Z.I., Manakos, I., Stathaki, T., Mucher, C.A., & Adamo, M. (2015b). Discrimination of Vegetation Height Categories With Passive Satellite Sensor Imagery Using Texture Analysis. *Ieee Journal of Selected Topics in Applied Earth Observations and Remote Sensing, 8*, 1442-1455

Phinn, S., Franklin, J., Hope, A., Stow, D., & Huenneke, L. (1996). Biomass distribution mapping using airborne digital video imagery and spatial statistics in a semi-arid environment. *Journal of Environmental Management, 47*, 139-164

Plourde, L.C., Ollinger, S.V., Smith, M.L., & Martin, M.E. (2007). Estimating species abundance in a northern temperate forest using spectral mixture analysis. *Photogrammetric Engineering and Remote Sensing, 73*, 829-840

Prabhakara, K., Hively, W.D., & McCarty, G.W. (2015). Evaluating the relationship between biomass, percent groundcover and remote sensing indices across six winter cover crop fields in Maryland, United States. *International Journal of Applied Earth Observation and Geoinformation, 39*, 88-102

Proctor, C., He, Y.H., & Robinson, V. (2013). Texture augmented detection of macrophyte species using decision trees. *Isprs Journal of Photogrammetry and Remote Sensing, 80*, 10-20

Rayburn, A.P., & Wiegand, T. (2012). Individual species-area relationships and spatial patterns of species diversity in a Great Basin, semi-arid shrubland. *Ecography, 35*, 341-347

Reddersen, B., Fricke, T., & Wachendorf, M. (2014). A multi-sensor approach for predicting biomass of extensively managed grassland. *Computers and Electronics in Agriculture, 109*, 247-260

Roberts, D.A., Dennison, P.E., Roth, K.L., Dudley, K., & Hulley, G. (2015). Relationships between dominant plant species, fractional cover and Land Surface Temperature in a Mediterranean ecosystem. *Remote Sensing of Environment, 167*, 152-167

Robinson, T.P., Wardell-Johnson, G.W., Pracilio, G., Brown, C., Corner, R., & van Klinken,

R.D. (2016). Testing the discrimination and detection limits of WorldView-2 imagery on a challenging invasive plant target. *International Journal of Applied Earth Observation and Geoinformation, 44*, 23-30

Rocchini, D., Andreo, V., Forster, M., Garzon-Lopez, C.X., Gutierrez, A.P., Gillespie, T.W., Hauffe, H.C., He, K.S., Kleinschmit, B., Mairota, P., Marcantonio, M., Metz, M., Nagendra, H., Pareeth, S., Ponti, L., Ricotta, C., Rizzoli, A., Schaab, G., Zebisch, M., Zorer, R., & Neteler, M. (2015). Potential of remote sensing to predict species invasions: A modelling perspective. *Progress in Physical Geography, 39*, 283-309

Roth, K.L., Dennison, P.E., & Roberts, D.A. (2012). Comparing endmember selection techniques for accurate mapping of plant species and land cover using imaging spectrometer data. *Remote Sensing of Environment, 127*, 139-152

Roth, K.L., Roberts, D.A., Dennison, P.E., Peterson, S.H., & Alonzo, M. (2015). The impact of spatial resolution on the classification of plant species and functional types within imaging spectrometer data. *Remote Sensing of Environment, 171*, 45-57

Sankey, J.B., Munson, S.M., Webb, R.H., Wallace, C.S.A., & Duran, C.M. (2015). Remote Sensing of Sonoran Desert Vegetation Structure and Phenology with Ground-Based LiDAR. *Remote Sensing, 7*, 342-359

Schaepman, M.E., Ustin, S.L., Plaza, A.J., Painter, T.H., Verrelst, J., & Liang, S.L. (2009). Earth system science related imaging spectroscopy-An assessment. *Remote Sensing of Environment, 113*, S123-S137

Schmidtlein, S., Feilhauer, H., & Bruelheide, H. (2012). Mapping plant strategy types using remote sensing. *Journal of Vegetation Science, 23*, 395-405

Shouse, M., Liang, L., & Fei, S.L. (2013). Identification of understory invasive exotic plants with remote sensing in urban forests. *International Journal of Applied Earth Observation and Geoinformation, 21*, 525-534

Sims, D.A., & Gamon, J.A. (2002). Relationships between leaf pigment content and spectral reflectance across a wide range of species, leaf structures and developmental stages. *Remote Sensing of Environment, 81*, 337-354

Stenzel, S., Fassnacht, F.E., Mack, B., & Schmidtlein, S. (2017). Identification of high nature value grassland with remote sensing and minimal field data. *Ecological Indicators, 74*, 28-38

Stock, W.D., Chuba, D.K., & Verboom, G.A. (2004). Distribution of South African C-3 and C-4 species of Cyperaceae in relation to climate and phylogeny. *Austral Ecology, 29*, 313-319

Suzuki, R. (2015). Assessment of terrestrial ecosystem function and service by remote

sensing. *Japanese Journal of Ecology (Otsu), 65*, 125-134

Tobler, M.W., Cochard, R., & Edwards, P.J. (2003). The impact of cattle ranching on large-scale vegetation patterns in a coastal savanna in Tanzania. *Journal of Applied Ecology, 40*, 430-444

Underwood, E.C., Ustin, S.L., & Ramirez, C.M. (2007). A comparison of spatial and spectral image resolution for mapping invasive plants in coastal California. *Environmental Management, 39*, 63-83

Ustin, S.L., & Gamon, J.A. (2010). Remote sensing of plant functional types. *New Phytologist, 186*, 795-816

Ustin, S.L., Roberts, D.A., Gamon, J.A., Asner, G.P., & Green, R.O. (2004). Using imaging spectroscopy to study ecosystem processes and properties. *Bioscience, 54*, 523-534

Van Aardt, J.A.N., & Wynne, R.H. (2007). Examining pine spectral separability using hyperspectral data from an airborne sensor: An extension of field-based results. *International Journal of Remote Sensing, 28*, 431-436

Wan, H.W., Wang, Q., Jiang, D., Fu, J.Y., Yang, Y.P., & Liu, X.M. (2014). Monitoring the Invasion of Spartina alterniflora Using Very High Resolution Unmanned Aerial Vehicle Imagery in Beihai, Guangxi (China). *Scientific World Journal*

Wang, T., Zhang, H.S., Lin, H., & Fang, C.Y. (2016). Textural-Spectral Feature-Based Species Classification of Mangroves in Mai Po Nature Reserve from Worldview-3 Imagery. *Remote Sensing, 8*, 15

White, D.C., Lewis, M.M., Green, G., & Gotch, T.B. (2016). A generalizable NDVI-based wetland delineation indicator for remote monitoring of groundwater flows in the Australian Great Artesian Basin. *Ecological Indicators, 60*, 1309-1320

Xian, G., Homer, C., Meyer, D., & Granneman, B. (2013). An approach for characterizing the distribution of shrubland ecosystem components as continuous fields as part of NLCD. *Isprs Journal of Photogrammetry and Remote Sensing, 86*, 136-149

Xian, G., Homer, C., Rigge, M., Shi, H., & Meyer, D. (2015). Characterization of shrubland ecosystem components as continuous fields in the northwest United States. *Remote Sensing of Environment, 168*, 286-300

Yemefack, M., Rossiter, D.G., & Njomgang, R. (2005). Multi-scale characterization of soil variability within an agricultural landscape mosaic system in southern Cameroon. *Geoderma, 125*, 117-143

Zhang, C.Y., & Qiu, F. (2012). Mapping Individual Tree Species in an Urban Forest Using

Airborne Lidar Data and Hyperspectral Imagery. *Photogrammetric Engineering and Remote Sensing, 78*, 1079-1087

Zhang, L., Li, X.S., Lu, S.L., & Jia, K. (2016). Multi-scale object-based measurement of arid plant community structure. *International Journal of Remote Sensing, 37*, 2168-2179

Supplementary Information

Chapter 1

Table S1 Point measurements for photosynthetic rate
Leaf-level seasonal gas exchange measurements (μmol m^{-2} s^{-1}) for 15 common species on the Colorado Plateau with the standard error values. Missing values indicate no tissue samples to measure.

Functional Type	Species	February	April	May	June	September	December
Grass	*Achnatherum hymenoides*			**10.9** (+/- 1.16 SE)	**11.52** (+/- 1.07 SE)	**1.36** (+/- 0.16 SE)	
	Bouteloua gracilis		**26.09** (+/- 0.19 SE)	**17.4** (+/- 1.92 SE)		**3.89** (+/- 0.80 SE)	
	Hesperostipa comata		**28.69** (+/- 0.49 SE)	**14.11** (+/- 2.11 SE)	**10.211** (+/- 0.49 SE)	**4.31** (+/- 0.01 SE)	
	Pleuraphis jamesii		**24.16** (+/- 0.55 SE)	**29.75** (+/- 0.86 SE)	**11.04** (+/- 0.55 SE)		
Shrub	*Chrysothamnus viscififlorus*	**0.84** (+/- 0.52 SE)	**19.86** (+/- 1.87 SE)	**14.04** (+/- 6.21 SE)	**16.75** (+/- 2.04 SE)	**5.31** (+/- 0.49 SE)	**1.89** (+/- 0.61 SE)
	Coleogyne ramosissima	**2.02** (+/- 0.37 SE)	**10.01** (+/- 1.22 SE)	**21.55** (+/- 2.69 SE)	**9.71** (+/- 0.91 SE)	**6.89** (+/- 0.40 SE)	**1.58** (+/- 0.54 SE)
	Ephedra viridis	**2.73** (+/- 0.32 SE)	**11.43** (+/- 0.39 SE)	**18.42** (+/- 3.11 SE)	**16.62** (+/- 1.19 SE)	**7.77** (+/- 0.39 SE)	**2.91** (+/- 0.94 SE)
Forb	*Amaranthus blitoides*			**10.87** (+/- 2.24 SE)	**15.2** (+/- 0.01 SE)		
	Astragalus amphioxys			**9.33** (+/- 2.14 SE)	**13.97** (+/- 0.55 SE)		
	Chenopodium album			**9.34** (+/- 3.17 SE)	**17.04** (+/- 0.80 SE)		
	Eriogonum inflatum			**3.97** (+/- 1.57 SE)			
	Lappula occidentalis		**11.63** (+/- 0.60 SE)	**18.19** (+/- 3.43 SE)			
	Lepidium densiflorum			**18.68** (+/- 0.89 SE)			
	Sphaeralcea coccinea			**10.14** (+/- 0.86 SE)			
	Streptanthella longirostris		**14.73** (+/- 1.33 SE)				

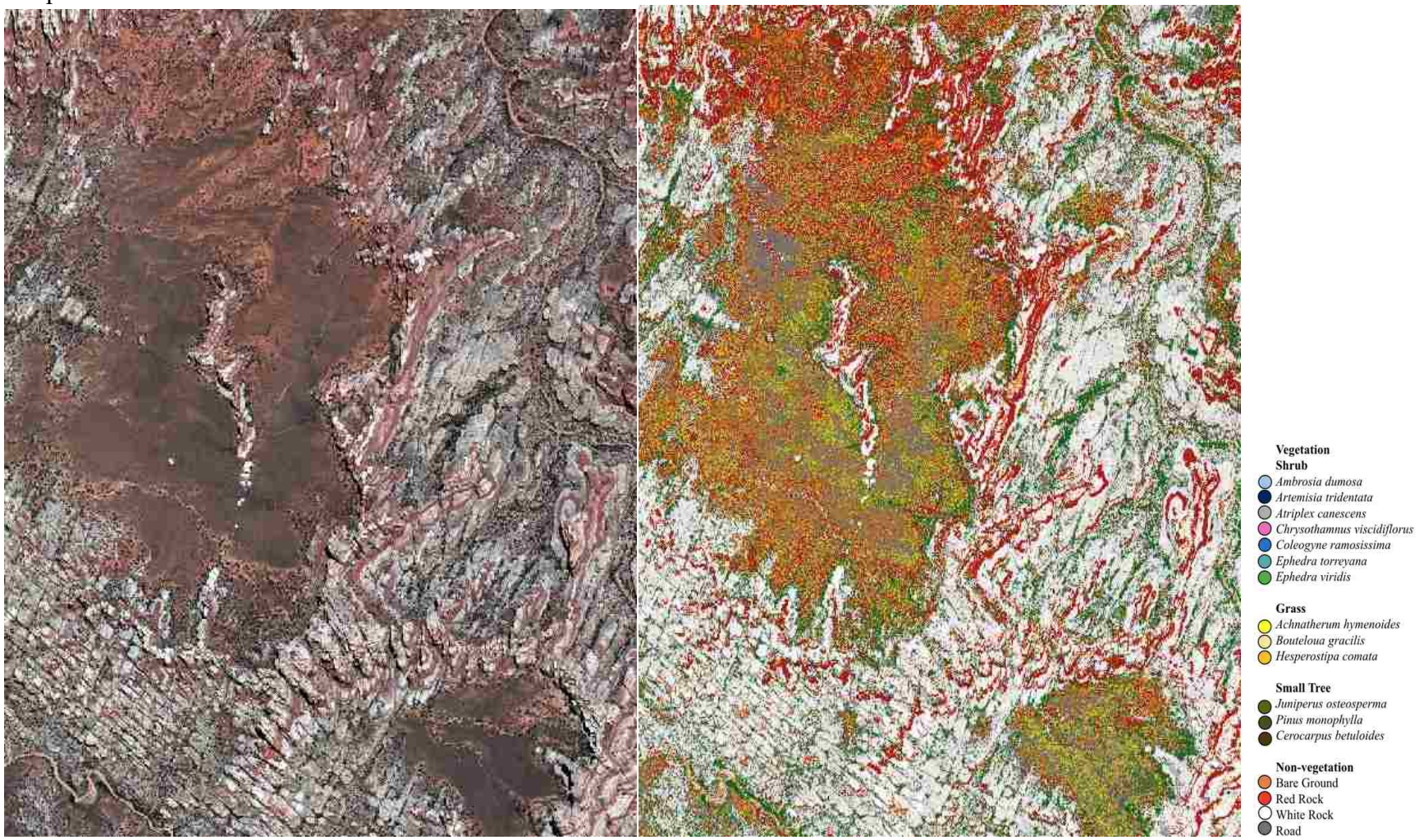

Figure S1 Original image and classification

Original image and classification using object oriented classification. The region pictured is of Chesler Park and Virginia Park, two canyon regions within Canyonlands National Park.

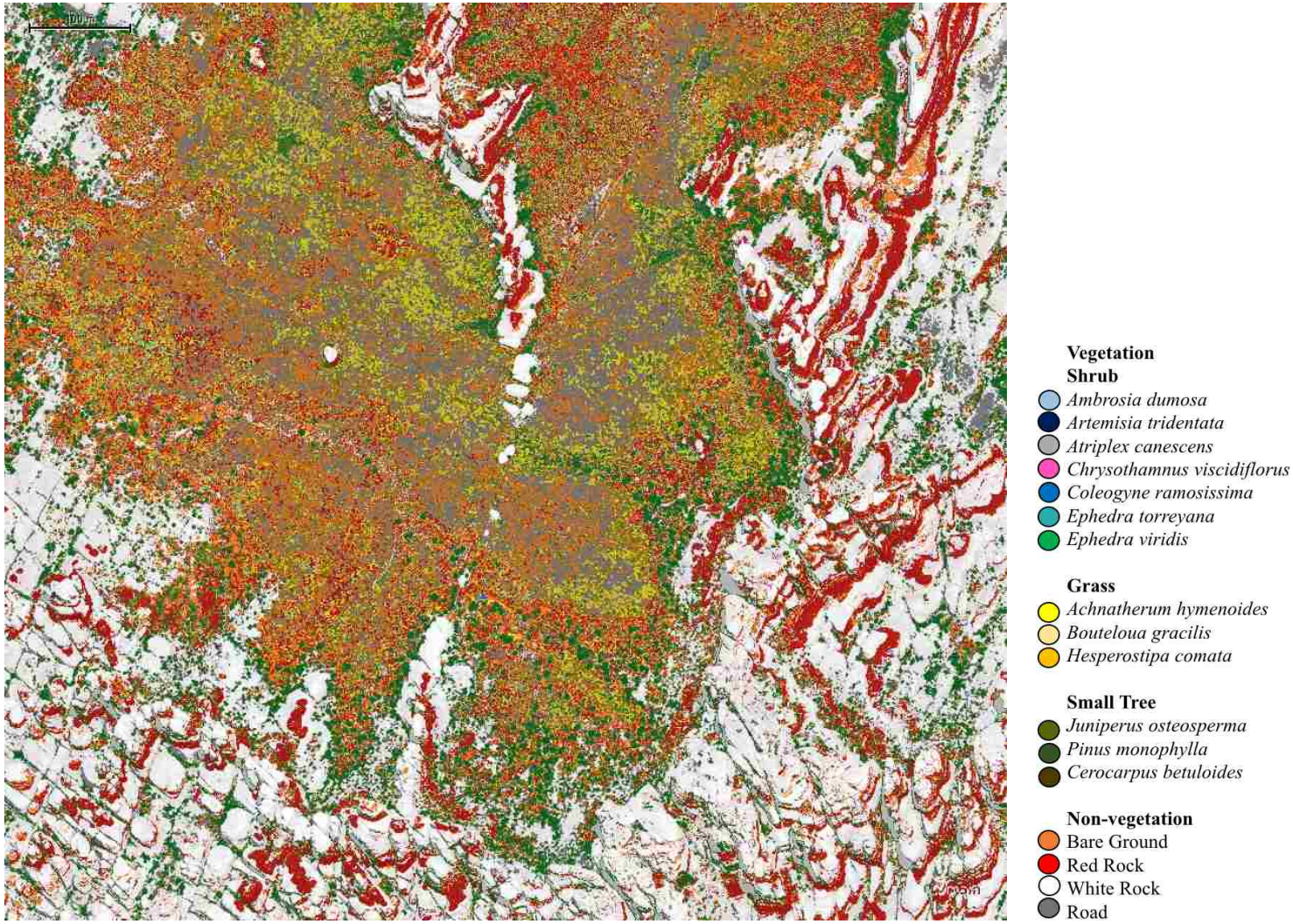

Figure S2 Chelser Park Classification

Close up image of Chesler Park classification. Visually, you can see the difference where the shrubs at the canyon walls meet the grasses within the basin.

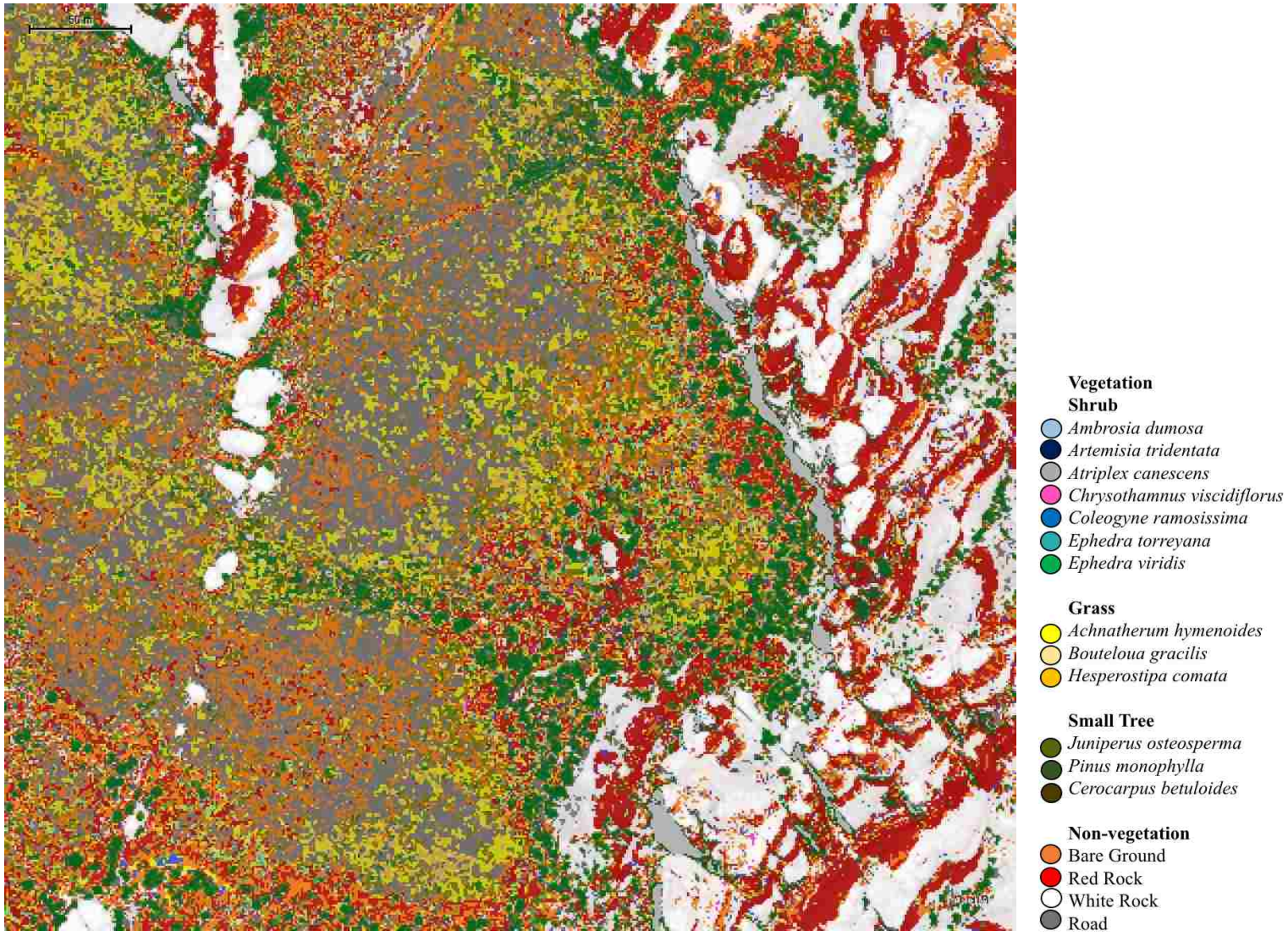

Figure S3 Zoomed in Chesler Park Classification
Smaller, more in-depth view of the classification of Chesler Park.

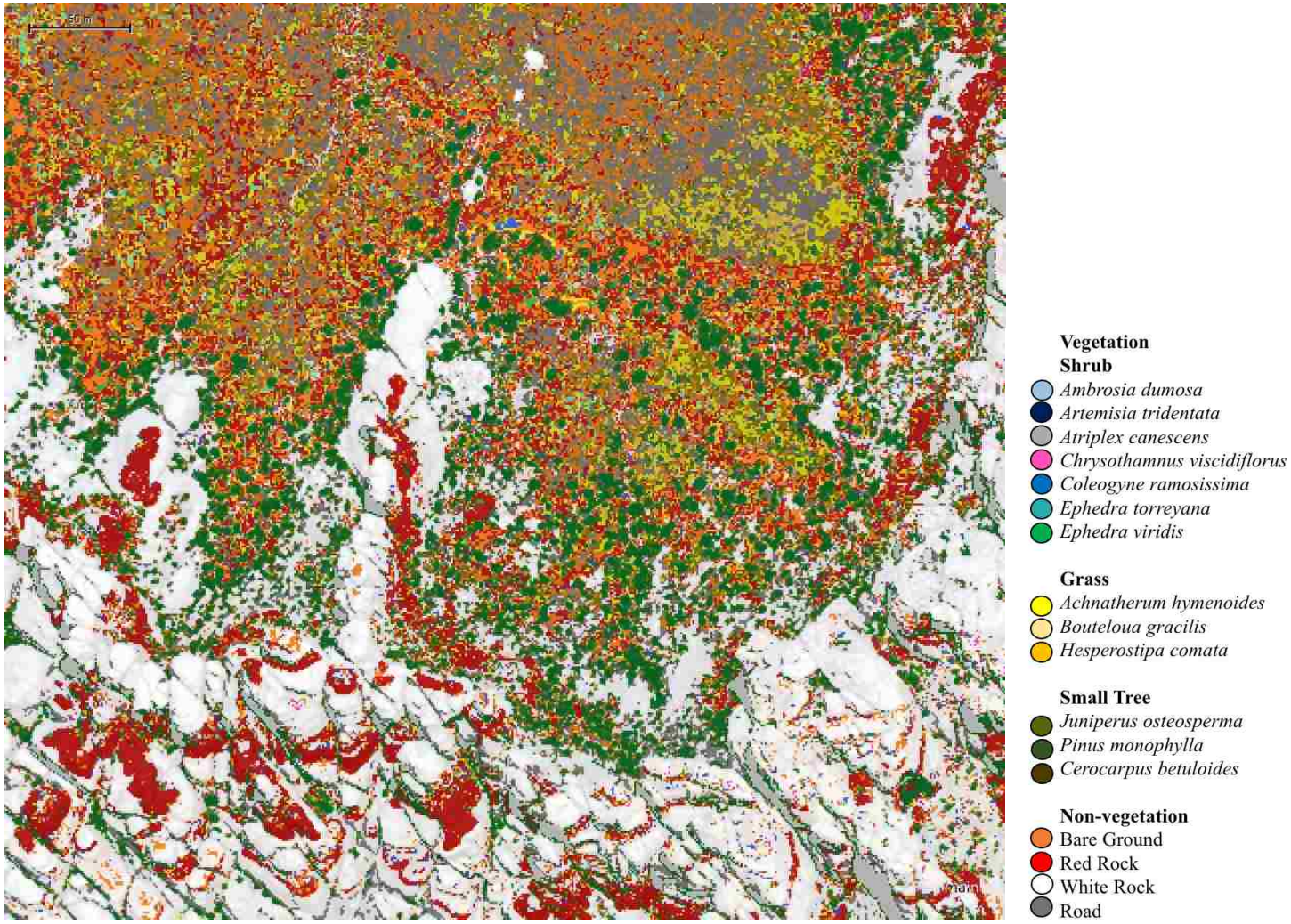

Figure S4 Shrub to grass interface in Chesler Park
Chesler Park detailed with the tree to shrub and shrub to grass interface with canyon geography.

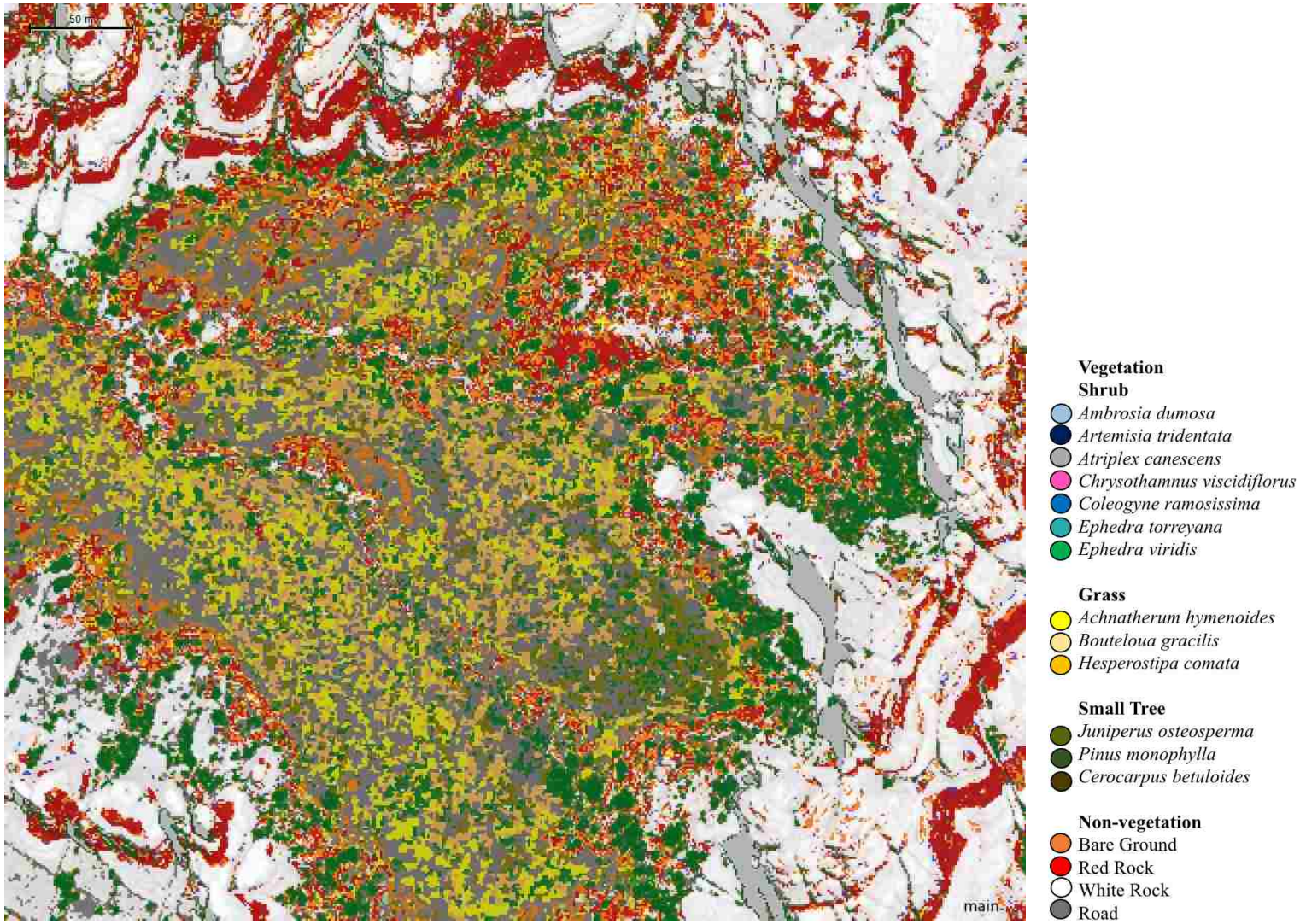

Figure S5 Virginia Park classification

Close up of Virginia Park, another canyon located near Chesler Park. Virginia Park differs from Chesler Park and other surrounding regions because it has never been grazed. The canyon is completely closed off to tourists and grazing animals so the plant community will likely vary from what is seen outside the canyon.

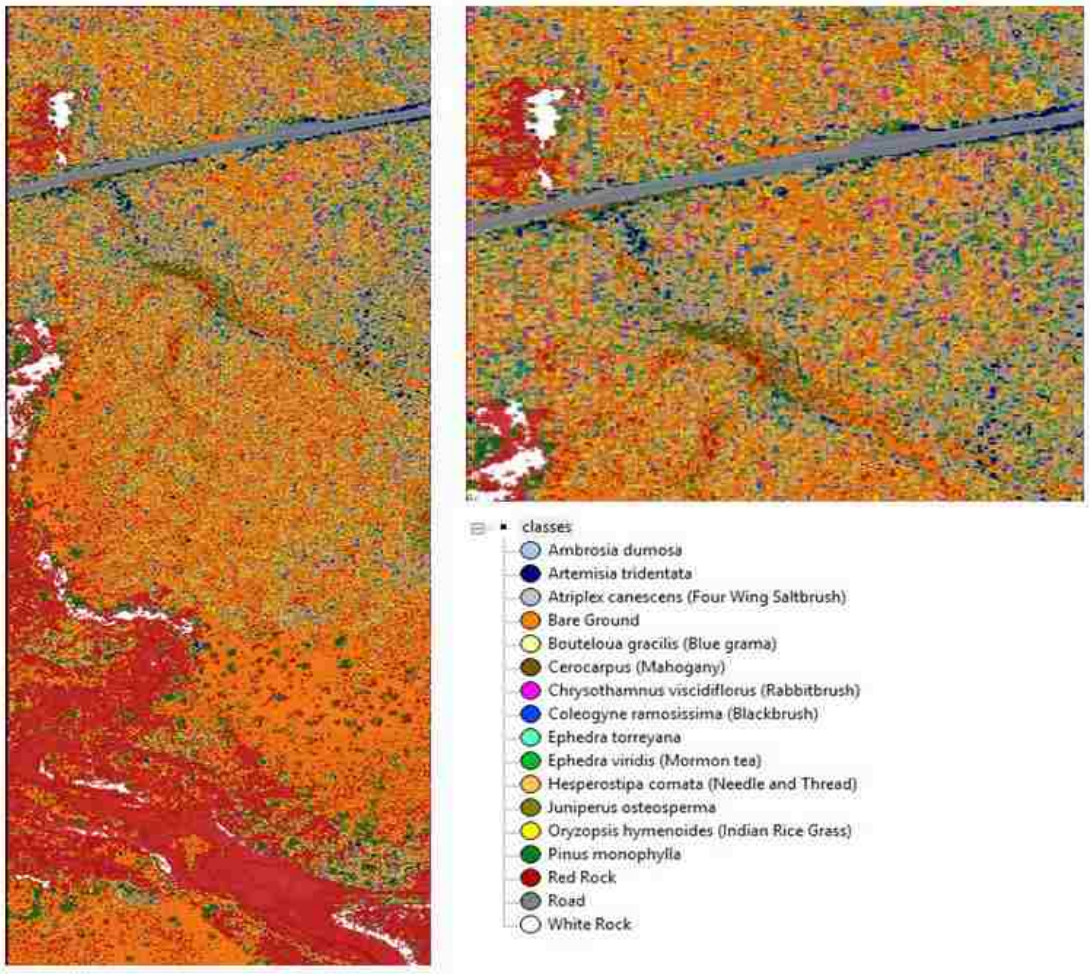

Figure S6 Visitor Center classification
Close-up of the front country area of the Needles District of Canyonlands National Park near the Visitor's Center.

Table S1 Classification Sample Editor

Table of Object Oriented Classification Sample Editors showing the overlap between parameters when comparing species.

Species	Overlap	Area	Thickness	Length/Thickness	Volume	Length/Width	Length	Number of Pixels	Relative border to image border	Width	Border length	Brightness	Mean Red	Mean NIR 1	Mean Green	Mean Blue	Mean NIR 2	Mean Coastal	Mean Red Edge	Mean Yellow	Max Difference	NDVI	GNDVI
Artemisia-Atriplex	0.86	1	1	0.86	0.71	0.71	0.86	1	1	0.86	0.21	0	0.02	0.18	0.54	0.07	0.49	0.24	0.14	0.33	0.52	0.31
Artemisia-Bare Ground	1	1	1	1	1	1	1	1	1	1	0	0	0.14	0	0.14	0.06	0.29	0	0	0.14	0.45	0.14
Artemisia-Bouteloua	0	0.14	0	0	0	0	0	0.14	0.14	0	0	0	0	0	0	0	0	0	0	0	0.1	0.03
Artemisia-Chrysothamnus	0	0.57	0.57	0	0	0	0	0.57	0.43	0	0	0	0.1	0	0	0	0	0	0	0.2	0.27	0
Artemisia-Coleogyne	0.14	0.29	0.29	0.14	0.14	0.29	0.14	0.29	0.14	0.29	0	0	0	0	0	0	0	0	0	0	0.04	0
Artemisia-Ephedra	0.71	1	1	0.71	0.57	0.57	0.71	1	1	0.71	0.14	0	0.11	0	0.14	0.14	0.17	0.14	0	0.1	0.63	0.44
Artemisia-Hesperostipa	1	1	1	1	1	1	1	1	1	1	0	0	0	0	0.02	0	0.25	0.08	0	0.14	0.34	0.19
Artemisia-Juniperus	1	1	1	1	0.86	0.86	1	1	1	0.86	0.52	0.94	0.26	1	1	0.3	0.79	0.29	1	0.2	0.39	0.26
Artemisia-Oryzopsis	0.71	1	1	0.71	0.57	0.86	0.71	1	1	0.71	0	0	0	0		0	0.29	0	0	0.14	0.29	0.14
Artemisia-Pinus	1	1	1	1	0.71	0.71	1	1	1	1	0.52	0.81	0.2	0.2	0.97	0.09	0.24	0.24	0.97	0.14	0.36	0.51
Atriplex-Bouteloua	0.05	0.05	0.05	0.05	0.05	0.05	0.05	0.05	0.05	0.05	0	0	0.3	0	0	0	0.5	0	0	0	0.03	0.04
Atriplex-Chrysothamnus	0.14	0.18	0.18	0.14	0.14	0.14	0.14	0.18	0.14	0.14	0.08	0.05	0.02	0.09	0.11	0.08	0.12	0.07	0.02	0.07	0.15	0.17
Atriplex-Coleogyne	0.05	0.09	0.09	0.05	0.05	0.05	0.05	0.09	0.09	0.09	0	0.2	0.07	0.03	0.05	0.3	0.04	0.04	0.04	0.09	0.01	0.08
Atriplex-Ephedra	0.68	0.73	0.73	0.68	0.68	0.68	0.68	0.73	0.68	0.68	0.4	0.15	0.19	0.44	0.38	0.43	0.46	0.35	0.44	0.32	-0.28	0.42
Atriplex-Hesperostipa	0.86	1	1	0.86	0.91	0.86	0.86	1	1	0.86	0.17	0.12	0.29	0.29	0.24	0.31	0.54	0.2	0.18	0.38	0.37	0.56
Atriplex-Juniperus	1	1	1	1	1	1	1	1	0.96	1	0.65	0.37	0.76	0.62	0.48	0.75	0.46	0.72	0.31	0.6	0.39	0.51
Atriplex-Oryzopsis	0.73	0.91	0.91	0.73	0.73	0.82	0.91	0.91	0.86	0.72	0.06	0	0.09	0.03	0.12	0.08	0.3	0.09	0.08	0.18	0.23	0.31
Atriplex-Pinus	1	1	1	1	1	1	1	1	1	1	0.42	0.14	0.6	27	0.13	0.58	0.06	0.64	0.13	0.29	0.18	0.39
Bouteloua-Chrysothamnus	1	1	1	1	1	1	1	1	1	1	0	0	0	1	0.8	0.3	0.28	0	0	0	0.55	0
Bouteloua-Coleogyne	0	1	1	0	0	0	0	1	1	0	0	0	0	0	0.9	0	0.72	0	0	0	0	0
Bouteloua-Ephedra	1	1	1	1	1	1	1	1	1	1	0	0	0	0	0.37	0	0.74	0	0	0.68	0.47	0.54
Bouteloua-Hesperostipa	1	1	1	1	1	1	1	1	1	1	0.19	0	1	1	1	1	1	0.75	1	0.88	1	1
Bouteloua-Juniperus	1	1	1	1	1	1	1	1	1	1	0.82	0	0.6	0	0	1	1	0	0	1	0	1
Bouteloua-Oryzopsis	1	1	1	1	1	1	1	1	1	1	1	1	0.61	1	1	0.66	1	0.4	1	1	0.82	1
Bouteloua-Pinus	1	1	1	1	1	1	1	1	1	1	0	0	0	0	0	0.19	0.33	0	0	1	0.2	1
Chrysothamnus-Coleogyne	0	0.5	0.5	0	0	0	0	0.5	0.25	0	0.2	0	0.07	0.07	0.41	0.13	0.17	0.25	0.14	0.02	0.07	0.38
Chrysothamnus-Ephedra	0.75	1	1	0.75	0.75	0.75	0.75	1	0.75	0.75	0.17	0.16	0.36	0.39	0.5	0.39	0.6	0.09	0.22	0.23	0.53	0.79
Chrysothamnus-Hesperostipa	0.75	1	1	0.75	0.75	0.75	0.75	1	0.75	1	0.55	0.42	0.75	1	1	0.88	0.85	0.75	0.5	0.88	1	1
Chrysothamnus-Juniperus	0.75	1	1	0.75	0.75	0.75	0.75	1	0.75	0.75	0.36	0.32	1	0.17	0	1	0.56	0.25	0.07	1	0.21	0.86
Chrysothamnus-Oryzopsis	0.75	1	1	0.75	0.75	0.75	0.75	1	0.75	0.75	0.3	0.4	0.2	0.43	1	0.25	0.75	0.25	0.25	0.44	0.5	0.54
Chrysothamnus-Pinus	0.75	1	1	0.75	0.75	0.75	0.75	1	0.75	0.75	0	0	0.55	0	0	0.97	0.1	0	0	0.85	0.05	0.64
Coleogyne-Ephedra	0	1	1	0	0	0	0	1	0.5	0.5	0.15	0	0.36	0.05	0.19	0.28	0.78	0.37	0	0.5	0.02	1
Coleogyne-Hesperostipa	0.6	1	1	0.5	1	1	0.5	1	1	1	1	1	0.28	1	1	0.88	0.85	0.92	0.89	0.73	1	0.97
Coleogyne-Juniperus	0.5	1	1	0.5	0.5	1	0.5	1	1	0.5	0.5	0	1	0	0	1	0.74	0.43	0.11	1	0	0.72
Coleogyne-Ozyzopsis	0	1	1	0	0.5	1	0	1	1	0.5	0	0.09	0	0.63	1	0	1	0.35	0.86	0.28	1	0.07
Coleogyne-Pinus	0.5	1	1	0.5	0.5	0.5	0.5	1	1	1	0	0	0.76	0.76	0	0	0.61	0	0	0.06	0	0.42
Ephedra-Hesperostipa	0.88	1	1	0.88	1	0.88	0.88	1	1	0.88	0.19	0.06	0.23	0.3	0.45	0.27	0.68	0.23	0.17	0.28	0.24	0.54
Ephedra-Juniperus	1	1	1	1	0.94	0.94	1	1	0.94	0.94	0.74	0.5	0.93	0.59	0.09	0.95	0.42	0.92	0.55	0.54	0.45	0.42
Ephedra-Ozyzopsis	0.88	1	1	0.88	0.81	0.81	0.99	1	0.94	0.88	0.03	0	0.08	0	0.16	0.06	0.27	0.03	0.06	0.14	0.13	0.16
Ephedra-Pinus	1	1	1	1	1	1	1	1	1	1	0.38	0.03	0.48	0.06	0	0.65	0.13	0.65	0.08	0.34	0.3	0.31
Hesperostipa-Juniperus	0.86	1	1	0.85	0.9	0.86	0.86	1	0.86	0.83	0.21	0.12	0.52	0.13	0.04	0.65	0.33	0.32	0.14	0.81	0.1	0.87
Hesperostipa-Oryzopsis	0.69	0.69	0.69	0.69	0.62	0.69	0.69	0.69	0.66	0.69	0.22	0.24	0.25	0.35	0.47	0.22	0.51	0.22	0.35	0.48	0.46	0.54
Hesperostipa-Pinus	0.83	1	1	0.83	0.86	0.79	0.83	1	0.93	0.83	0.01	0	0.47	0.02	0	0.4	0.07	0.03	0	0.53	0.07	0.51
Juniperus-Oryzopsis	0.21	0.23	0.23	0.21	0.2	0.23	0.21	0.23	0.21	0.2	0.02	0.01	0.06	0	0	0.1	0.06	0.03	0.02	0.22	0.02	0.23
Juniperus-Pinus	0.59	0.59	0.59	0.59	0.58	0.58	0.59	0.59	0.57	0.58	0.43	0.4	0.41	0.5	0.47	0.37	0.46	0.44	0.43	0.4	0.34	0.51
Oryzopsis-Pinus	0.9	1	1	0.9	0.85	0.9	0.9	1	0.95	0.9	0	0	0.18	0	0	0.24	0.05	0	0	0.64	0.1	0.71